Synthesis, Structure, and Reactivity of η^2-N_2-Aryldiazoalkane Titanium Complexes: Cleavage of the N−N Bond

Anne W. Kaplan,[†] Jennifer L. Polse,[†] Graham E. Ball,[‡] Richard A. Andersen,*[,†] and Robert G. Bergman*[,†]

Contribution from the Department of Chemistry, University of California, Berkeley, California 94720, and School of Chemistry, The University of New South Wales, 2052 Sydney, Australia

Received April 20, 1998

Abstract: A series of η^2-N_2-titanium aryldiazoalkane complexes $Cp^*_2Ti(N_2CHAr)$ (**5**−**10**), where Ar is a *para*-substituted aryl group, have been prepared by addition of aryldiazoalkanes to $Cp^*_2Ti(C_2H_4)$ (**4**). Unlike most diazoalkane complexes, they release dinitrogen thermally to give transient carbene complexes which may be trapped with styrene to form the titanacyclobutane complexes $Cp^*_2Ti(CHArCHPhCH_2)$ (**11**−**15**). The kinetics of these reactions in toluene-d_8 at 78.0 °C have been examined by ^{1}H NMR spectroscopy. A Hammett analysis ($\rho = -0.26$) indicated that the reaction is relatively insensitive to *para*-substituents on the aromatic ring of the diazoalkane ligand, but application of the *E*- and *C*-based dual parameter substituent constant analysis suggests that this may be due to almost exactly compensating covalent and electrostatic contributions of each substituent to the reaction rate. The stability of the aryldiazoalkane complexes at temperatures below 75 °C allows their reactivity to be explored without competitive N_2 loss. The addition of ^{t}BuNC results in a coordination change of the diazoalkane fragment from η^2 to η^1 to give $Cp^*_2Ti(\eta^1\text{-}N_2CHPh)(^t\text{BuNC})$ (**16**), as shown by ^{15}N NMR chemical shifts and N−H coupling constants. The bound ^{t}BuNC ligand exchanges with free ^{t}BuNC in solution, as established by an EXSY experiment. Trineopentylaluminum coordinates to the terminal nitrogen atom on the diazoalkane fragment to form $Cp^*_2TiN(AlNp_3)N(C(H)C_6H_4Me)$ (**17**), as determined by X-ray crystallography. Silanes ($HSiR_3$; $R_3 = PhH_2$, Ph_2H) add across the Ti−N bond of $Cp^*_2Ti(N_2C(H)C_6H_4Me)$ to give (*E*)-$Cp^*_2Ti(H)(N(SiR_3)(N{=}C(H)C_6H_4Me)$ ((*E*)-**19**, (*E*)-**20**), the kinetic product and (*Z*)-$Cp^*_2Ti(H)(N(SiR_3)(N{=}C(H)C_6H_4Me)$ ((*Z*)-**19**, (*Z*)-**20**), the thermodynamic product. Diazoalkane adduct $Cp^*_2Ti(N_2C(H)C_6H_4Me)$ undergoes N−N bond cleavage when treated with CO to form an alkylideneimido isocyanato complex $Cp^*_2Ti(NCO)N{=}C(H)C_6H_4Me)$ (**21**).

Introduction

Diazoalkane complexes have been implicated as intermediates in the synthesis of metal carbene complexes from organic diazoalkanes[1−5] and in the metal catalyzed cyclopropanation of olefins by diazoalkanes (eq 1).[3,4,6−9]

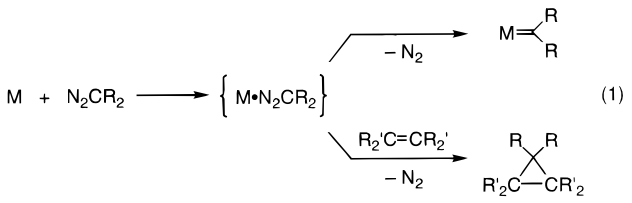

(1)

However, the mechanism of dinitrogen loss from organic diazoalkanes at a metal center is still largely unknown.[4] The majority of known metal diazoalkane complexes involve η^1-coordination to the metal center and are resistant to N_2 loss[10] due to stabilization of the diazoalkane ligand by metal coordination;[1,4] however, other coordination modes are possible. The reactivity of these coordinated diazoalkane ligands is affected by their coordination mode and thus is often different from that of the free diazoalkane.[1] Also of interest is the relevance of diazoalkane complexes as models in the chemistry of N_2 fixation.[11−14]

We recently reported the synthesis and chemistry of $Cp^*_2TiN_2C(H)SiMe_3$ (**1**), an example of an η^2-N_2-titanium diazoalkane complex that undergoes facile N_2 loss at room temperature to generate a transient carbene complex **2** which may be trapped by alkenes, including styrene, to form titanacyclobutane complex **3** (Scheme 1). These studies were limited because N_2 is lost from **1** at room temperature.[15] We now describe a general method for preparing the more thermally stable aryldiazoalkane complexes. Their unusual and widely varied reactivity patterns

[†] University of California, Berkeley.
[‡] University of New South Wales.

(1) Sutton, D. *Chem. Rev.* **1993**, *93*, 995.
(2) Schwab, P.; Grubbs, R. H.; Ziller, J. W. *J. Am. Chem. Soc.* **1996**, *118*, 100.
(3) Mizobe, Y.; Ishii, Y.; Hidai, M. *Coord. Chem. Rev.* **1995**, *139*, 281.
(4) Herrmann, W. A. *Angew. Chem., Int. Ed. Engl.* **1978**, *17*, 800.
(5) Aggarwal, V. K.; Ford, J. G.; Thompson, A.; Jones, R. V. H.; Standen, M. C. H. *J. Am. Chem. Soc.* **1996**, *118*, 7004.
(6) Herrmann, W. A.; Menjon, B.; Herdtweck, E. *Organometallics* **1991**, *10*, 2134.
(7) Doyle, M. P.; Peterson, L. S.; Zhou, Q. L.; Nishiyama, H. *Chem. Commun.* **1997**, 211, and references cited therein.
(8) Doyle, M. P.; Peterson, C. S.; Parker, D. L., Jr. *Angew. Chem., Int. Ed. Engl.* **1996**, *35*, 1334.
(9) Maxwell, J. L.; Brown, K. C.; Bartley, D. W.; Kodadek, T. *Science* **1992**, *256*, 1544.
(10) Clauss, A. D.; Shapley, J. R.; Wilson, S. R. *J. Am. Chem. Soc.* **1981**, *103*, 7387.
(11) Hidai, M.; Mizobe, Y. *Chem. Rev.* **1995**, *95*, 1115.
(12) Kisch, H.; Holzmeier, P. *Adv. Organomet. Chem.* **1992**, *34*, 67.
(13) Sellmann, D. *Angew. Chem., Int. Ed. Engl.* **1974**, *13*, 639.
(14) Chatt, J. *J. Organomet. Chem.* **1975**, *100*, 17.
(15) Polse, J. L.; Andersen, R. A.; Bergman, R. G. *J. Am. Chem. Soc.* **1996**, *118*, 8737.

10.1021/ja981340b CCC: $15.00
Published on Web 11/03/1998

Scheme 1

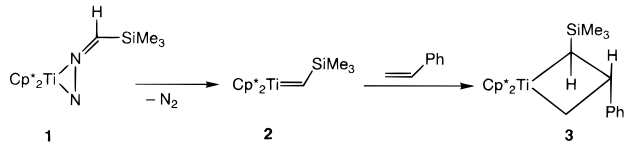

Scheme 2

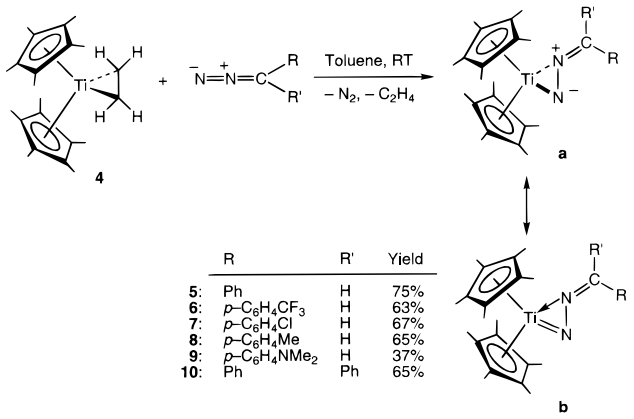

	R	R'	Yield
5:	Ph	H	75%
6:	*p*-$C_6H_4CF_3$	H	63%
7:	*p*-C_6H_4Cl	H	67%
8:	*p*-C_6H_4Me	H	65%
9:	*p*-$C_6H_4NMe_2$	H	37%
10:	Ph	Ph	65%

will be presented, including transformations that result in N−N bond fission of the diazoalkane fragment. Mechanistic studies on the loss of N_2 from titanium aryldiazoalkane complexes will also be discussed.

Results

Synthesis and Characterization of Aryldiazoalkane Complexes. Treatment of a toluene or benzene solution of $Cp^*_2Ti(C_2H_4)$ (**4**) with 1 equiv of aryldiazomethane results in gas evolution and an immediate color change from lime to forest green. Removal of the solvent gives dark green powders that may be crystallized from toluene at −50 °C to give pure **5**−**10** in 60−80% yield (Scheme 2). Retention of the nitrogen atoms in **5**−**10** was confirmed by mass spectroscopy, elemental analysis and X-ray crystallography for **5** and **9**. The spectroscopic data for **5**−**10** are similar. For example, the ^{1}H NMR spectrum of **8** displays singlets at δ 2.19 and 1.67 ppm for the aryl methyl and equivalent Cp* methyl groups, respectively. In addition, there is a singlet at δ 5.46 ppm that is assigned to the methine proton of the diazoalkane ligand. The $^{13}C\{^1H\}$ NMR spectrum shows a methine resonance at δ 106.9 ppm for the N-bound carbon in the diazoalkane ligand.

It was previously shown that the diazoalkane fragment in $Cp^*_2TiN_2C(H)SiMe_3$ (**1**) is coordinated in an η^2-N_2 fashion. Because of the wide variety of possible coordination modes for diazoalkane ligands, it is often difficult to predict their structures based on spectroscopic data. We therefore used single-crystal X-ray diffraction to determine the coordination mode of the aryldiazoalkane ligands in two more examples, adducts **5** and **9**. An ORTEP diagram of **5** is shown in Figure 1, crystal and data collection parameters are given in Table 1, and representative bond lengths and angles are given in Table 2. Details of the structure determination are provided in the Experimental Section and as Supporting Information. Because of the disorder observed in **5** (see Supporting Information for a picture and details of the disorder model used), the bond lengths and angles about the Ti−N−N are artificially lengthened. The structural study clearly shows, however, that the aryldiazoalkane fragment is bound to the titanium center in a side-on fashion through the two nitrogen atoms. Although side-on coordination is less common than end-on or bridging coordination modes, it is not unprecedented.[1,3,4,16−18]

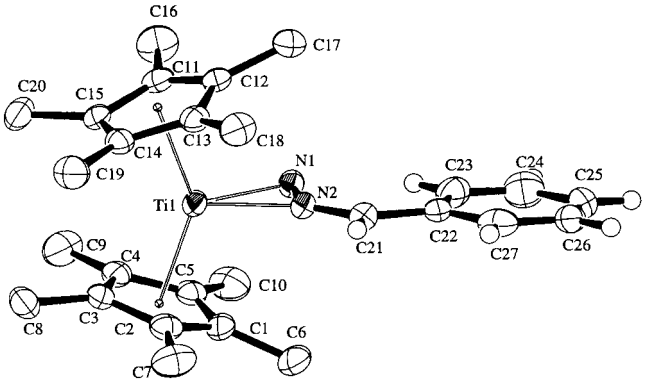

Figure 1. ORTEP diagram of $Cp^*_2TiN_2C(H)C_6H_5$ (**5**). The disorder in the diazoalkane group, which superimposes the two orientations of the N1 and N2 Ar fragments, is not shown. See Supporting Information for the full disorder model.

Better information about the bond lengths and angles about the Ti−N−N core were obtained on the analogous diazoalkane complex **9**. An ORTEP diagram is shown in Figure 2, crystal and data collection parameters are given in Table 1, and representative bond lengths and angles are given in Table 3. Details of the structure determination are provided in the Experimental Section and as Supporting Information. The aryldiazoalkane ligand is bound to the titanium in an η^2-N_2 fashion, and the distances for Ti−N1 (1.97(1) Å) and Ti−N2 (1.99(1) Å) in **9** are indicative of single bonds and are similar to those found for the trimethylsilyldiazoalkane adduct **1** (1.979(2) and 2.012(2) Å, respectively). The structures of both **5** and **9** show that the arene rings point into (in an *E* configuration), rather than away from, the wedge of the metallocene, which we have found to affect the reactivity of these complexes (vide infra).

Thermal N_2 Loss from Aryldiazoalkane Complexes in the Presence of Styrene: Preparation of Titanacyclobutane Complexes. Unlike complex **1**, which is thermally unstable at room temperature, **5**−**9** are stable to 75 °C. When **5**−**9** are heated to 75 °C for 1 day in the presence of styrene, the metallacycles **11**−**15** are formed in isolated yields of about 50% (eq 2). The ^{1}H NMR spectra of the metallacycles show the

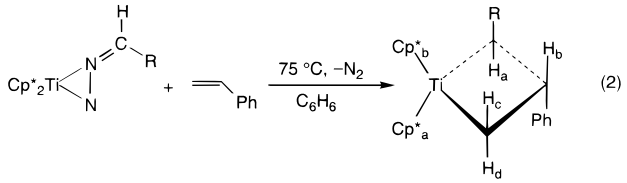

(2)

R = Ph (**11**), *p*-$C_6H_4CF_3$ (**12**), *p*-C_6H_4Cl (**13**), *p*-C_6H_4Me (**14**), *p*-$C_6H_4NMe_2$ (**15**)

expected features, including inequivalent Cp* ligands. Formation of **11**−**15** is regio- and stereospecific, since only one isomer is observed by NMR spectroscopy; this behavior is similar to that observed for the addition of alkenes to $Cp^*_2Ti(N_2CHSiMe_3)$ (**1**).[19] The metallacycle formed from styrene was identified as the α,β-disubstituted isomer by a combination of one- and two-

(16) Schramm, K. D.; Ibers, J. A. *Inorg. Chem.* **1980**, *19*, 2441.
(17) Gambarotta, S.; Floriani, C.; Chiesi-Villa, A.; Guastini, C. *J. Am. Chem. Soc.* **1982**, *104*, 1918.
(18) Nakamura, A.; Yoshida, T.; Cowie, M.; Otsuka, S.; Ibers, J. A. *J. Am. Chem. Soc.* **1977**, *99*, 2108.
(19) Polse, J. L.; Kaplan, A. W.; Andersen, R. A.; Bergman, R. G. *J. Am. Chem. Soc.* **1998**, *120*, 6316.

Table 1. Crystal Data for **5** and **9**

	5	**9**
diffractometer	Siemens Smart	Siemens Smart
T (°C)	−97.0	−111.0
radiation	Mo Kα (λ = 0.710 69 Å)	Mo Kα (λ = 0.710 69 Å)
take-off angle (deg)	6.0	6.0
cryst-to-detec dist (mm)	60	60
cryst color, habitat	black blocklike	red blocky clusters
cryst size (mm)	0.22 × 0.28 × 0.38	0.10 × 0.11 × 0.17
cryst syst	primitive monoclinic	primitive monoclinic
reflcns used for unit cell refinement	6054	3003
scan rate (s/frame)	10.0	20.0
$2\theta_{max}$ (deg)	52.0	52.1
no. of reflcns collected	11 112	6475
no. of unique reflcns	4298	2534
R_{int}	0.041	0.050
no. of obsd reflcns	2832	1583
$I > 3.00\sigma(I)$		
no. of variables	279	156
reflcns/param ratio	10.15	10.15
R	0.044	0.091
R_w	0.055	0.108
goodness of fit	1.88	3.26
p-factor	0.03	0.03
max shift/error in final cycle	0.01	0.90
max and min peaks in final diff map ($e^-/Å^3$)	+0.33/−0.39	+0.54/−0.49

Table 2. Selected Bond Distances (Å) and Angles (deg) for **5**

Ti−N1	2.004(3)	Ti−N2	2.001(2)
Ti−Cp*1[a]	2.0864(5)	Ti−Cp*2	2.0966(5)
N1−N2	1.236(4)	N2−C21	1.348(4)
C21−C22	1.449(5)		
Cp*1−Ti−Cp*2	142.80(3)	N1−Ti−Cp*1	106.68(9)
N1−Ti−Cp*2	108.08(9)	N2−Ti−Cp*1	109.17(8)
N2−Ti−Cp*2	106.65(7)	N1−Ti−N2	36.0(1)
Ti−N2−C21	152.7(3)	N1−N2−C21	135.1(3)
N2−C21−C22	124.1(3)	Ti−N1−N2	71.9(2)

[a] Cp* is the ring centroid of the Me_5C_5 ring.

Table 3. Selected Bond Distances (Å) and Angles (deg) for **9**

Ti−N1	1.97(1)	Ti−N2	1.99(1)
Ti−Cp*1[a]	2.0044(6)	Ti−Cp*2	2.1758(4)
N1−N2	1.29(1)	N2−C1	1.30(2)
C1−C2	1.47(2)		
Cp*1−Ti−Cp*2	141.67(8)	N1−Ti−Cp*1	112.29(5)
N1−Ti−Cp*2	104.58(6)	N2−Ti−Cp*1	109.61(6)
N2−Ti−Cp*2	105.72(3)	N1−Ti−N2	37.9(4)
Ti−N2−C1	156.9(9)	N1−N2−C1	132(1)
N2−C1−C2	127(1)	Ti−N1−N2	71.8(6)

[a] Cp* is the ring centroid of the Me_5C_5 ring.

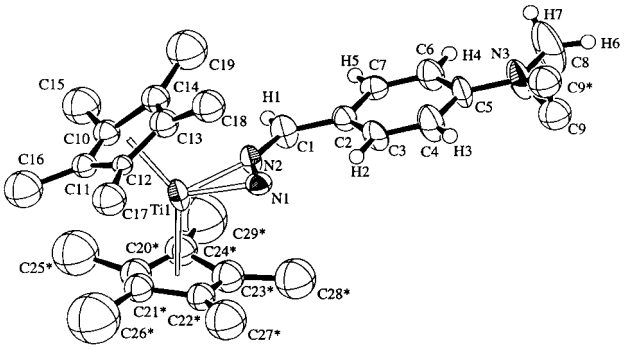

Figure 2. ORTEP diagram of $Cp^*_2TiN_2C(H)C_6H_4NMe_2$ (**9**). Asterisks indicate positional disorder in the atoms.

dimensional NMR techniques and X-ray crystallography.[20] The ^{13}C NMR spectrum shows methylene group resonances for **11**−**15** between 76 and 77 ppm, typical for a titanium-bound carbon and consistent with those observed in the metallacycles formed from **1**. The stereochemistry was determined using $^1H-^1H$ NOESY and one-bond $^1H-^{13}C$ HMQC[21] methods; spectra are included for **14** in the Supporting Information. When diphenyldiazoalkane complex **10** is treated with styrene, no reaction is observed up to 135 °C, at which point decomposition to multiple products occurs.

Mechanistic Studies on the Loss of N_2 from Organic Diazoalkanes at a Metal Center. We have previously reported kinetic studies on the reaction of $Cp^*_2Ti(N_2CHSiMe_3)$ (**1**) with styrene in toluene-d_8, which leads to the titanacyclobutane complex **3** (Scheme 1). The reaction rate was independent of styrene concentration and rigorously first-order in **1**; over a temperature range of 30−60 °C, $\Delta H^‡ = 22.5 \pm 0.3$ kcal/mol, $\Delta S^‡ = -3.1 \pm 1.0$ eu, and $\Delta G^‡ = 23.4 \pm 0.4$ kcal/mol (calculated at 25 °C). Formation of the metallacyclobutane complex **3** was proposed to occur via a rate-limiting formation of carbene intermediate **2** followed by [2 + 2] cycloaddition with the olefin (Scheme 1).[15] To assess whether a significant charge buildup occurs in the transition state, the rate of formation of **3** from **2** was measured in the more polar solvent, THF-d_8. No rate change was observed. We therefore undertook a detailed study of the electronic factors influencing dinitrogen loss from the phenyl-substituted diazoalkane complexes to probe the nature of the transition state more closely.

The kinetics of the reaction of aryldiazoalkane complex **8** with styrene in toluene-d_8 at 78.0 °C to form **14** have been examined by ^1H NMR spectroscopy. To ensure that the observed rate constants would be independent of the concentration of styrene, the styrene concentration used was 10 times greater than the concentration of **8**. A typical plot of concentration vs time is shown in Figure 3. The observed rate constant was found to be independent of styrene concentration, as was the case for **1**. The reaction follows first-order kinetics to greater than five half-lives. We have carried out a Hammett σ/ρ study using aryldiazoalkane complexes having CF_3 (**6**), Cl (**7**), H (**5**), Me (**8**), and NMe_2 (**9**) substituents in the *para*-positions of the aromatic ring (Figure 4). This provides a large electronic range,

(20) For a description of the methods used to assign regio- and stereochemistry in titanacyclobutane complexes, see ref 19.

(21) Bax, A.; Subramanian, S. *J. Magn. Reson.* **1986**, *67*, 565.

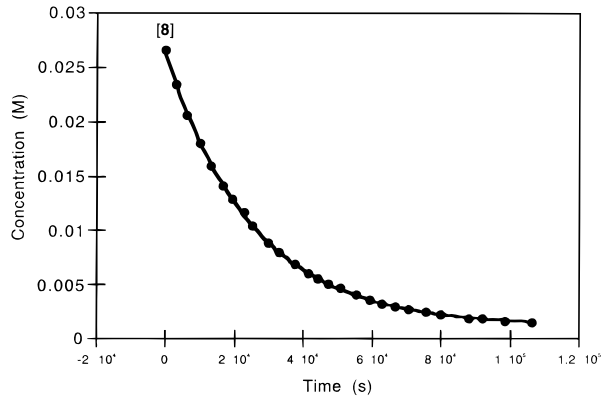

Figure 3. Plot of concentration vs time and exponential fit for the formation of **14** from **8** and styrene at 78.0 °C (where, for example, $-2\ 10^4 = -2 \times 10^4$).

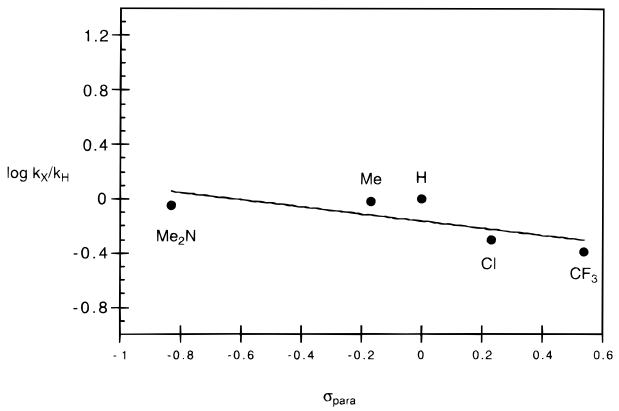

Figure 4. Hammett plot and linear fit for the reaction of *p*-X-aryldiazoalkane complexes with styrene where X = Me_2N, Me, H, Cl, or CF_3.

and a linear log *k* vs σ_{para} plot was obtained. The ρ obtained for the reaction was -0.26, indicating that the reaction rate is relatively insensitive to the electron-donating or -withdrawing character of the *para*-substituents on the aromatic ring. Further analysis by applying the *E*- and *C*-base dual parameter substituent correlation method is presented in the Discussion.

Reaction of Phenyldiazoalkane Complex 5 with ^{t}BuNC. The addition of a Lewis base, ^{t}BuNC, induces a coordination change of the diazoalkane fragment from η^2 to η^1, giving deep red crystals of **16** in 72% yield (Scheme 3). The IR spectrum of **16** shows a stretch at 2139 cm^{-1} for the C≡N bond in the isonitrile ligand. A singlet in the ^{1}H NMR spectrum at 1.88 ppm shows that the Cp* methyl groups are equivalent, which eliminates the possibility that **16** is a diazirine complex with ^{t}BuNC bound to titanium, which would have inequivalent Cp* methyls. The proton on the diazoalkane fragment is shifted about 1 ppm downfield, to 6.48 ppm, relative to that in **5**. Likewise, the N-bound carbon on the diazoalkane fragment is deshielded 15 ppm in the isonitrile adduct. Exposure of solutions of **16** to vacuum for periods of time greater than 1 h results in loss of ^{t}BuNC, regenerating the diazoalkane complex **5**. In the ^{1}H NMR spectrum, the bound ^{t}BuNC at 1.14 ppm in **16** exchanges with free ^{t}BuNC even though the two resonances are distinct at 50 °C. Exchange was established by observing cross-peaks between the bound and free ^{t}BuNC resonances at 50 °C in an EXSY experiment (Figure 5). On the basis of the above data, complex **16** is assigned the structure shown in Scheme 3.

It is unlikely that **16** still possesses a side-bound diazoalkane ligand with the ^{t}BuNC coordinated to the metal, since this would

Scheme 3

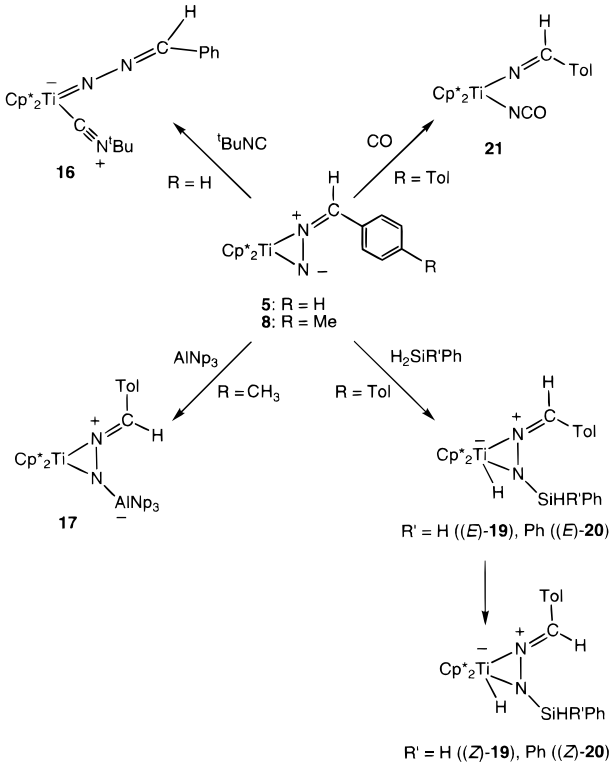

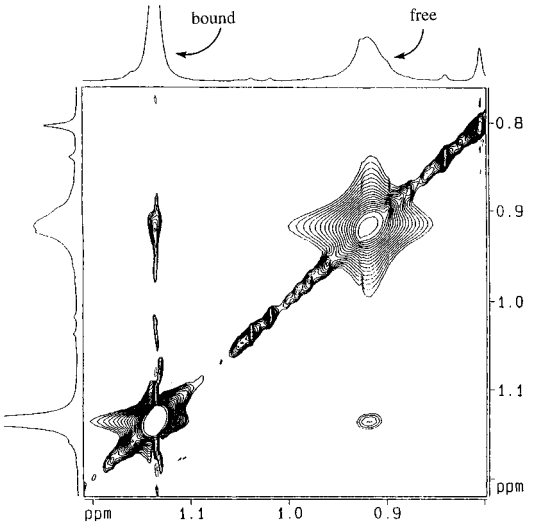

Figure 5. EXSY spectrum of ^{t}Bu resonances in $Cp^*_2Ti(^t$BuNC)(N_2-CHPh) (**16**) and free ^{t}BuNC.

result in steric crowding around the bulky decamethyltitanocene fragment. Analysis by ^{15}N NMR spectroscopy is potentially useful for providing an answer to the structural dilemma.[22−27] The ^{15}N shifts for the ^{t}BuNC adduct **16**, as well as the diazoalkane adduct **5**, and their coupling constants were determined on the natural abundance compound by taking advantage of the ^{1}H−^{15}N scalar coupling. The ^{1}H−^{15}N cor-

(22) Levy, G. C.; Lichter, R. L. *Nitrogen-15 NMR Spectroscopy*; Wiley-Interscience: New York, 1979; pp 1−221.
(23) Martin, G. J.; Martin, M. L.; Gouesnard, J.-P. *^{15}N NMR Spectroscopy*, NMR Basic Principles Program: New York, 1981; Vol. 18, pp 1−382.
(24) Witanowski, M.; Stefaniak, L.; Webb, G. A. *Annu. Rep. NMR Spectrosc.* **1986**, *18*, 1−761.
(25) Haymore, B. L.; Hughes, M.; Mason, J.; Richards, R. L. *J. Chem. Soc., Dalton Trans.* **1988**, 2935.
(26) Mason, J. *Chem. Rev.* **1981**, *81*, 205.
(27) Mason, J. *Chem. Rev.* **1987**, *87*, 1299.

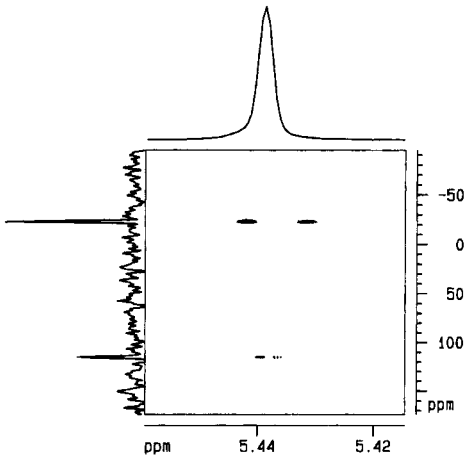

Figure 6. Fast HSQC spectrum of Cp*$_2$Ti(η^2-N$_2$CHPh) (**5**) at 298 K. Annotated with proton spectrum in F_2 and a single column through cross-peaks in F_1.

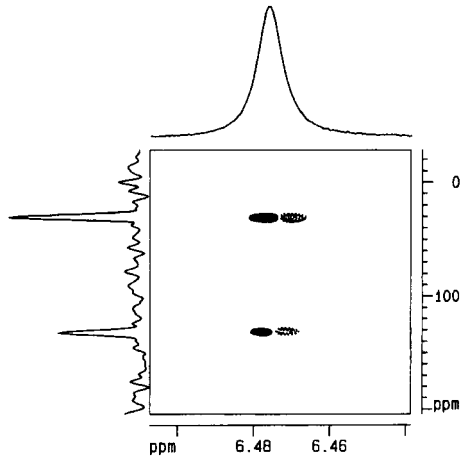

Figure 7. Fast HSQC spectrum of Cp*$_2$Ti(CN^{t}Bu)(η^1-N$_2$CHPh) (**16**) at 298 K. Annotated with proton spectrum in F_2 and a single column through cross-peaks in F_1.

relation spectra for diazoalkane adduct **5** (Figure 6) and **16** (Figure 7) were recorded using a modified fast HSQC sequence.[28] Details of the experiment are provided in the Experimental Section. The ^{15}N shifts (and N−H coupling constants) for **5** are −23.1 ppm (6.3 Hz) and 115.2 ppm (1.5 Hz). The ^{15}N shifts (and N−H coupling constants) for **16** are 30 ppm (3.5 Hz) and 132 ppm (2.9 Hz). Assignment of the shifts to individual nitrogen atoms cannot be made from the limited amount of data. The downfield resonances may correspond to the carbon-bound nitrogen since ^2J values are typically less than ^3J values, but the difference in absolute values of the coupling constants is small so this argument is not compelling.[29] It is more reasonable that the downfield resonances correspond to the nitrogen that remains coordinated to the titanium center. The shift of the terminal nitrogen in organic diazoalkanes is typically downfield from the central nitrogen shift.[30] The larger change in chemical shift for the nitrogen that goes from bound (−23 ppm, **5**) to free (30 ppm, **16**), $\Delta\delta$ = 53 ppm, as compared to the nitrogen which is connected to the titanium center in both complexes (115 ppm in **5** and 132 ppm in **16**), $\Delta\delta$ = 17 ppm, is also consistent with this assignment. Generally, the largest contribution to chemical shift changes is due to changes in geometry, i.e., from linear to bent.[25,27] However, both nitrogen atoms change geometry in going from **5** to **16**, so the largest change is apparent in the most deshielded nitrogen, as a consequence of decoordination from the titanium center.

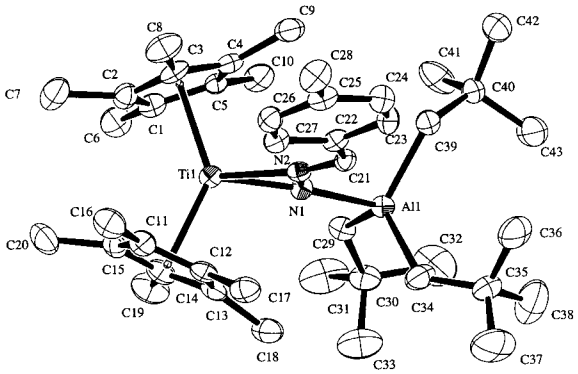

Figure 8. ORTEP diagram of Cp*$_2$TiN(Al(CH$_2$CMe$_3$)$_3$)N(C(H)C$_6$H$_4$-Me) (**17**).

Reaction of Tolyldiazoalkane Complex 8 with a Lewis Acid. Since the titanium center in **5** is Lewis acidic, we were interested in determining if the diazoalkane fragment has Lewis basic sites. The addition of a Lewis acid (trineopentylaluminum) results in coordination to the terminal nitrogen on the diazoalkane fragment (Scheme 3). When a benzene solution of **8** is treated with Np$_3$Al for 1 day, the solution turns from dark green to deep red. Removal of the volatile materials and crystallization from toluene (−50 °C) gives crystals of **17** in 62% yield (Scheme 3). Mass spectroscopy and elemental analysis confirm the retention of nitrogen. The ^{1}H NMR spectrum shows the expected resonances for the tolyl group and a singlet for the equivalent Cp* methyl groups. The proton on the diazoalkane fragment is shifted far downfield to 7.80 ppm. A crystal structure shows that Al is bound to the terminal nitrogen, as shown in Figure 8. Crystal and data collection parameters are shown in Table 4. Table 5 lists selected bond lengths and angles. Details of the structure determination are given in the Experimental Section, and the positional and thermal parameters are given as Supporting Information. The Np$_3$Al group is bound to the terminal nitrogen on the diazoalkane fragment, with the tolyl group rotated away from the metallocene wedge and away from the bulky neopentyl groups. The N1−N2 distance was found to be 1.327(5) Å, lengthened from that of **5** or **9** by 0.10 and 0.04 Å, respectively.

Imido-like Reactivity of a Titanium Diazoalkane Complex: Addition of Silanes. The N−N bond of titanium aryldiazoalkane complexes is single and polar, as shown in Scheme 2. The resonance structure **b** emphasizes the double bond character of the titanium−nitrogen bond, and previous studies have shown that the trimethylsilyldiazoalkane complex **1** reacts in an "imido-like fashion" by undergoing cycloaddition reactions with terminal alkynes and allene.[19] We were interested in further exploring the "imido-like" character of the diazoalkane fragment in the aryl series. The authentic imido complex, Cp*$_2$-Ti=NPh (**18**), reacts with dihydrogen to form the corresponding amido hydride Cp*$_2$Ti(H)(NHPh).[31] In contrast, addition of an atmosphere of dihydrogen to a benzene solution of **8** results in decomposition, but silanes add across the Ti−N bond. Addition of PhSiH$_3$ to a benzene solution of **8** resulted in a color change from dark green to olive green to yellow. Removal of the benzene and crystallization from ether yields (*Z*)-**19** in 78% yield

(28) Mori, S.; Abeygunawardana, C.; Johnson, M. O.; Vanzijl, P. C. M. *J. Magn. Reson., B* **1995**, *108*, 94.
(29) Förster, H. G.; Roberts, J. D. *J. Am. Chem. Soc.* **1980**, *102*, 6984.
(30) Mason, J.; Vinter, J. G. *J. Chem. Soc., Dalton Trans.* **1975**, 2522.
(31) Smith, M. R., III; Ball, G. E.; Andersen, R. A. Manuscript in preparation.

Table 4. Crystal Data for **17**, (*Z*)-**19**, and **21**

	17	(*Z*)-**19**	**21**
diffractometer	Siemens Smart	Siemens Smart	Siemens Smart
T (°C)	−99.0	−110.0	−105.0
radiation	Mo Kα (λ = 0.716 09 Å)	Mo Kα (λ=0.710 69 Å)	Mo Kα (λ=0.710 69 Å)
take-off angle (deg)	6.0	6.0	6.0
cryst-to-detec dist (mm)	60	60	60
cryst color, habitat	orange plate-shaped	yellow irregular	clear orange blocks
cryst size (mm)	0.32 × 0.19 × 0.05	0.20 × 0.28 × 0.30	0.18 × 0.24 × 0.33
cryst syst	primitive triclinic	primitive monoclinic	orthorhombic
reflcns used for unit cell refinmt	3457	7594	5694
scan rate (s/frame)	10.0	10.0	10.0
$2\theta_{max}$ (deg)	52.3	52.2	52.1
no. of reflcns collected	11 583	14 570	12 325
no. of unique reflcns	7099	5807	2683
R_{int}	0.058	0.034	0.061
no. of obsd reflcns $I > 3.00\sigma(I)$	3838	3650	3263
no. of variables	424	355	297
reflcns/param ratio	9.05	10.28	10.99
R	0.067	0.042	0.047
R_w	0.064	0.047	0.047
goodness of fit	1.85	1.49	1.60
p-factor	0.03	0.03	0.03
max shift/error in final cycle	0.00	0.00	0.00
max and min peaks in final diff map ($e^-/Å^3$)	+0.46/−0.39	+0.41/−0.34	+0.30/−0.37

Table 5. Selected Bond Distances (Å) and Angles (deg) for **17**

Ti−N1	1.989(4)	Ti−N2	2.027(4)
Ti−Cp*1[a]	2.115(1)	Ti−Cp*2	2.107(1)
N1−N2	1.328(5)	N2−C21	1.304(6)
C21−C22	1.465(7)	N1−Al	2.023(4)
Cp*1−Ti−Cp*2	136.62(5)	N1−Ti−Cp*1	111.8(1)
N1−Ti−Cp*2	109.9(1)	N2−Ti−Cp*1	108.3(1)
N2−Ti−Cp*2	111.4(1)	N1−Ti−N2	38.6(1)
Ti−N2−C21	161.0(4)	N1−N2−C21	129.5(4)
N2−C21−C22	124.1(5)	Ti−N1−N2	72.2(3)
Ti−N1−Al	162.8(2)	Al−N1−N2	124.9(3)

[a] Cp* is the ring centroid of the Me_5C_5 ring.

(Scheme 3). Mass spectroscopy and elemental analysis confirm the elemental composition for (*Z*)-**19**, and the IR spectrum shows Si−H stretches at 2168 and 2097 cm^{-1}. The ^1H NMR spectrum exhibits the expected tolyl resonances, a singlet for the equivalent Cp* methyl groups, and a singlet at 5.63 ppm attributable to the protons on silicon. Silicon satellites are observable for this resonance (J_{HSi} = 207.8 Hz). The proton on the diazoalkane fragment and the titanium hydride resonate at 8.06 and 3.54 ppm, respectively.

To confirm the NMR deduction, a single-crystal X-ray diffraction study was undertaken, and an ORTEP diagram is shown in Figure 9. The structure was solved by direct methods and refined using standard least squares and Fourier techniques. Crystal and data collection parameters are shown in Table 4, and selected bond lengths and angles are shown in Table 6. Details of the structure determination are given in the Experimental Section, and positional and thermal parameters are given as Supporting Information. As can be seen in the ORTEP diagram, the aryl groups on the silicon and on the diazoalkane fragment are pointing away from the metallocene wedge, most likely to minimize steric interactions. The N1−N2 bond distance of 1.357(3) Å is slightly longer (0.03 Å) than in **17**. The hydrogens on the titanium and silicon were located in the difference map and refined with isotropic temperature factors. The Ti−H distance is 1.64(3) Å, and the hydride is coplanar with the Ti−N1−N2 core.

When the reaction of **8** with $PhSiH_3$ is followed by ^1H NMR spectroscopy in benzene-d_6, an intermediate assigned to the

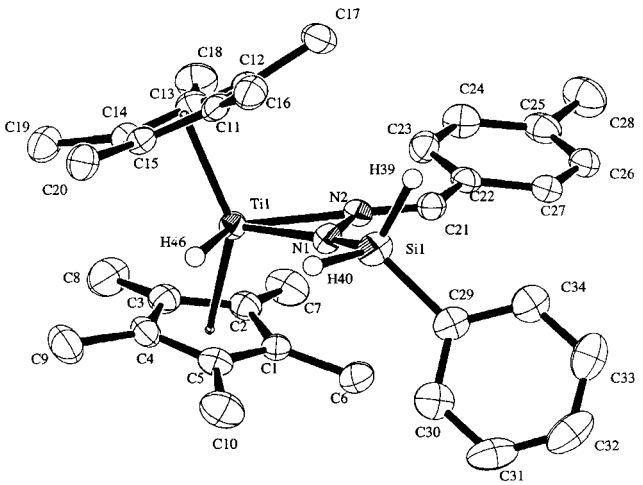

Figure 9. ORTEP diagram of (*Z*)-Cp*$_2$Ti(H)(N(SiH$_2$Ph)(NC(H)C$_6$H$_4$-Me) ((*Z*)-**19**). The hydrogen atoms on Si and Ti were refined with isotropic thermal parameters.

Table 6. Selected Bond Distances (Å) and Angles (deg) for (*Z*)-**19**

Ti−N1	2.054(2)	Ti−N2	2.177(2)
Ti−Cp*1[a]	2.1267(5)	Ti−Cp*2	2.1135(5)
N1−N2	1.357(3)	N2−C21	1.297(3)
C21−C22	1.461(4)	Si−N1	1.720(2)
Si−C29	1.872(3)		
Cp*1−Ti−Cp*2	138.92(3)	N1−Ti−Cp*1	110.22(7)
N1−Ti−Cp*2	110.80(7)	N2−Ti−Cp*1	106.24(6)
N2−Ti−Cp*2	107.40(6)	N1−Ti−N2	37.28(8)
Ti−N2−C21	168.1(2)	N1−N2−C21	124.6(2)
N2−C21−C22	125.9(3)	Ti−N1−N2	76.29(1)
Ti−N1−Si	155.1(1)	Si−N1−N2	127.2(2)

[a] Cp* is the ring centroid of the Me_5C_5 ring.

isomer (*E*)-**19** is observed within 10 min at room temperature and the color of the solution at this time is olive green. The intermediate (*E*)-**19** is converted to the final product (*Z*)-**19** over the course of 2 days, and the color of the solution is now yellow-orange. Complexes (*E*)-**19** and (*Z*)-**19** have similar ^1H NMR spectra. In particular, the resonance of the proton on the diazoalkane fragment shifts from 7.40 ppm in (*E*)-**19** to 8.06

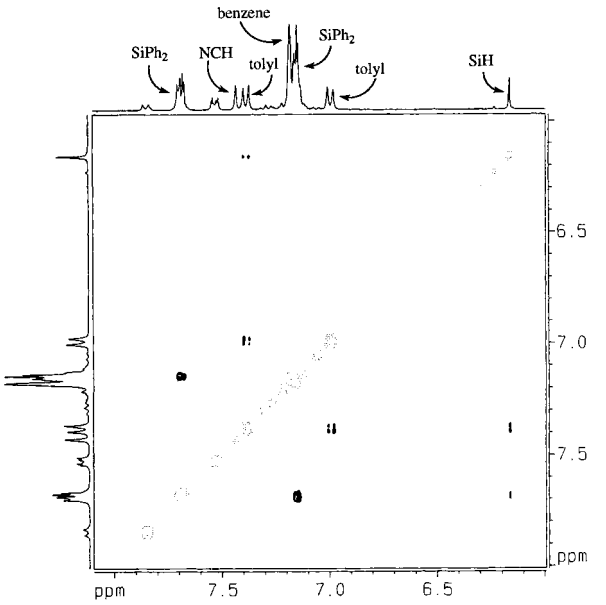

Figure 10. NOESY spectrum of (*E*)-**20**.

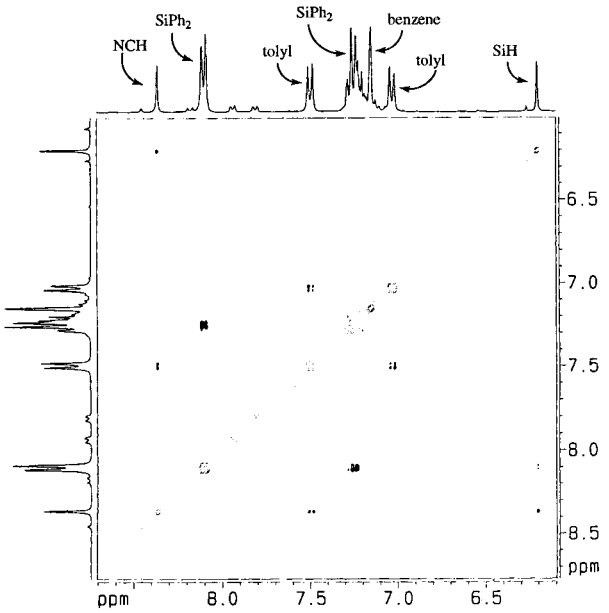

Figure 11. NOESY spectrum of (*Z*)-**20**.

ppm in (*Z*)-**19**. It is assumed that the intermediate (*E*)-**19** is the product of kinetically controlled addition of silane across the Ti−N bond of **5** and then the tolyl group on the diazoalkane fragment rotates out of the wedge to form the less sterically congested and therefore stable isomer (*E*)-**19** (Scheme 3). In this way the environments of the diazoalkane protons will result in different chemical shifts.

Both the rate of addition of silane to **8** and the rate of the ensuing isomerization can be decreased by using Ph_2SiH_2. Using this silane allows the intermediate *E*-isomer to be isolated. Treatment of **8** with Ph_2SiH_2 in benzene for 3 days results in a color change from dark green to olive green. Removal of the solvent gives an olive green powder which may be crystallized from ether to give (*E*)-**20** in 54% yield (Scheme 3). When the same reaction is performed for a longer period of time, 17 days, the reaction solution turns yellow. Removal of the solvent and crystallization from ether gives (*Z*)-**20** in 52% yield (Scheme 3). Mass spectroscopy and elemental analysis confirm the elemental composition of (*Z*)-**20**. The IR spectrum shows Si−H stretches at 2140 and 2094 cm^{-1} for (*Z*)-**20**. The ^{1}H NMR spectra are similar, the major difference being that the resonance of the proton on the diazoalkane fragment is shifted from 7.40 ppm in (*E*)-**20** to 8.37 ppm in (*Z*)-**20**. To determine whether (*E*)-**20** and (*Z*)-**20** are indeed isomers differing only in the relative positions of the tolyl group and proton on the diazoalkane ligand, ^{1}H-^{1}H NOESY spectra were acquired as described in the Experimental section. The NOESY spectra of (*E*)-**20** (Figure 10) and (*Z*)-**20** (Figure 11) were acquired. For the kinetic product (*E*)-**20**, cross-peaks are observed between the silicon hydride and the protons on the tolyl group. No NOE's are observed between the silicon hydride and the proton on the diazoalkane fragment, consistent with the orientation of these groups in the *E*-isomer. In the case of the *Z*-isomer, the silicon hydride resonance shows no NOE's to the tolyl group protons, but cross-peaks are observed between the silicon hydride resonance and the proton on the diazoalkane fragment. This is consistent with the orientation of these groups in the *Z*-configuration.

Reaction of Tolyldiazoalkane Complex 8 with CO: Cleavage of the N−N Bond. Perhaps the most intriguing reaction of **8** is with CO. Exposure of **8** to an atmosphere of CO in benzene at room temperature for 2 days yields the isocyanate

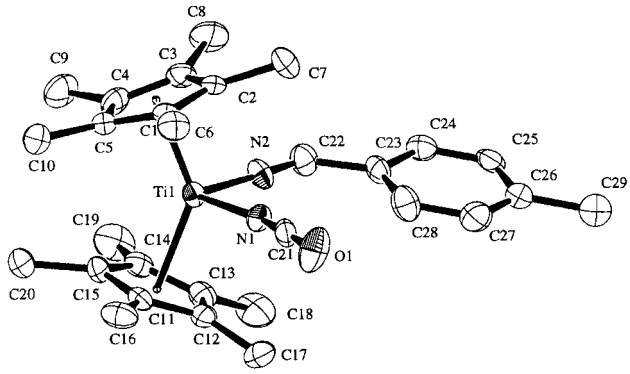

Figure 12. ORTEP diagram of Cp*$_2$Ti(NCO)(N=C(H)C$_6$H$_4$Me) (**21**).

21 as yellow crystals in 87% yield (Scheme 3). Retention of both nitrogen atoms was confirmed by mass spectroscopy and elemental analysis. The ^{1}H NMR spectrum of **21** shows a singlet for the equivalent Cp* methyl groups, resonances for a tolyl group, and a downfield shift of the proton on the diazoalkane fragment to 8.64 ppm. The ^{13}C{^{1}H} NMR spectrum shows a drastic downfield shift of the carbene carbon of the diazoalkane fragment from 106.9 ppm in diazoalkane adduct **8** to 155.2 ppm in **21**. A new quaternary carbon resonance at 120.6 ppm is observed. The IR spectrum contains a strong stretch at 2215 cm^{-1}. The above data are consistent with the formulation of **21** as Cp*$_2$Ti(NCO)N=C(H)C$_6$H$_4$Me), Scheme 3.

To confirm that the N−N bond in **21** was cleaved, a single crystal X-ray diffraction study was undertaken. The ORTEP diagram is shown in Figure 12, Table 7 lists selected bond lengths and angles, and crystal and data collection parameters are shown in Table 4. Details of the structure determination are given in the Experimental Section, and positional and thermal parameters are given as Supporting Information. The crystal structure determination clearly shows that the N−N bond was cleaved, resulting in formation of an isocyanato and an alkylideneimido ligand.

When the above reaction was monitored by ^{1}H NMR spectroscopy in benzene-d_6, an intermediate was observed immediately after the addition of CO and the solution color turned from green to red. In an effort to isolate this intermediate,

Table 7. Selected Bond Distances (Å) and Angles (deg) for **21**

Ti−N1	2.072(4)	Ti−N2	1.888(4)
Ti−Cp*1[a]	2.1228(5)	Ti−Cp*2	2.1116(5)
N1−C21	1.156(6)	N2−C22	1.258(6)
O−C21	1.222(6)	C22−C23	1.487(6)
Cp*1−Ti−Cp*2	139.83(3)	N1−Ti−Cp*1	102.40(11)
N1−Ti−Cp*2	102.13(11)	N2−Ti−Cp*1	104.39(12)
N2−Ti−Cp*2	103.49(11)	N1−Ti−N2	97.24(16)
Ti−N2−C22	178.7(4)	N2−NC22−C23	126.1(5)
O−C21−N1	179.5(5)	Ti−N1−N2	168.9(4)

[a] Cp* is the ring centroid of the Me_5C_5 ring.

Scheme 4

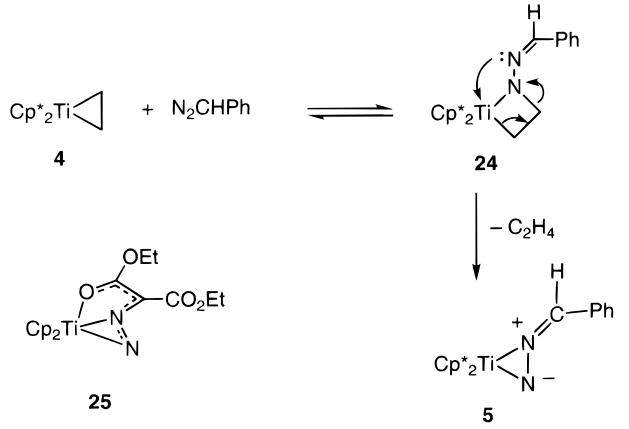

the volatile materials were removed in vacuo after 10 min at room temperature, but upon concentration, the solution turned from red to green and >95% **8** was recovered. It is likely that the intermediate is $Cp^*_2Ti(CO)(N_2C(H)C_6H_4Me)$ (**22**), similar to the aforementioned ^{t}BuNC adduct **16**. Upon exposure to a dynamic vacuum, the weakly bound CO dissociates.

Discussion

Synthesis and Stability of Aryldiazoalkane Complexes. As described in Results, treatment of **4** with organic aryldiazoalkanes results in clean formation of diazoalkane complexes **5**−**10** and ethylene (Scheme 2). A possible mechanism for the formation of **1** was outlined earlier,[15] and a similar pathway is suggested for the formation of **5**−**10** in Scheme 4. Thus the diazoalkane inserts into the Ti−C bond of **4** forming an azametallacyclobutane complex **24**, which cycloreverts to liberate ethylene and form the diazoalkane complex **5**. Examples of both steps have been documented[32,33] and discussed.[19] The possibility of ethylene dissociation followed by diazoalkane coordination seems to be unlikely since ethylene does not dissociate from **4** at room temperature.[34]

One significant difference between the preparation of the trimethylsilyl derivative **1** and the aryl derivatives **5**−**10** is that the latter are much less sensitive to reaction time and temperature. This stems from the fact that while the formation of diazoalkane complexes in the decamethyltitanocene system is fast, the products themselves have differing stabilities toward loss of dinitrogen. The trimethylsilyldiazoalkane adduct **1** loses dinitrogen at room temperature, whereas the monoaryl derivatives **5**−**9** are stable to 75 °C and the diphenyldiazoalkane complex **10** is stable to 135 °C. The loss of dinitrogen presumably gives a carbene complex intermediate which is trapped with alkenes to form titanacyclobutane complexes (Scheme 1, eq 2). Even with the higher temperature required to release dinitrogen from **5**−**9**, clean formation of titanacyclobutanes is observed.

The complexes **1** and **5**−**9** are unusual since they lose N_2, unlike the majority of diazoalkane complexes described in the literature.[1,4] For example, the related titanium diazoalkane complexes Cp_2Ti(DEDM) (**25**, Scheme 4) and $Cp_2Ti(\eta^1\text{-}N_2\text{-}CPh_2)(PMe_3)$ (**26**) do not lose dinitrogen thermally or photochemically.[17,35] Our mechanistic studies (vide infra) suggest that an open coordination site on the titanium center is necessary for dinitrogen loss. This explains why **25** and **26** do not lose dinitrogen whereas the complexes of type $Cp^*_2Ti(N_2CRR')$ do. In the latter cases, the diazoalkane fragment occupies two coordination sites, leaving one open on the titanium center. Additionally, the diazoalkane fragment can change coordination from η^2 to η^1 (vide infra). Metals are frequently used to induce decomposition of organic diazo compounds; the rhodium- or copper-catalyzed cyclopropanation of alkenes is a familiar example.[7,9] The active intermediates in these reactions are thought to be metal carbene complexes that are formed from a diazoalkane complex, although these intermediates are not observed. Though less common, some examples of isolated diazoalkane complexes which lose dinitrogen to give a metal carbene complex have been described.[3,10,16,18,36−38] In the titanocene system, the preparation of diazoalkane adducts is general and their thermal loss of dinitrogen is clean, which has enabled us to study the mechanism of this important transformation in detail (vide infra).

Reaction of Monoaryldiazoalkane Complexes 5−9 with Styrene. Mechanistic Discussion. A kinetic study of the reaction of **1** with styrene was performed previously, and the proposed mechanism involves an initial rate-determining loss of dinitrogen to give a carbene complex intermediate **2** which then in a fast step undergoes a [2 + 2] cycloaddition with the alkenes to give metallacyclobutane complexes (Scheme 1).[15] The availability of the more thermally stable aryldiazoalkane series **5**−**9** allowed us to investigate the distribution of charge in the rate-determining (N_2-loss) transition state. A Hammett study was performed in which the *para*-substituents of the aryl ring on the diazoalkane fragment were varied. A relatively linear Hammett correlation was obtained, but the very small ρ value of −0.26 showed that the rate is not strongly affected by either strongly electron-withdrawing or electron-donating groups.

The conventional interpretation of this apparent insensitivity of the rate to changes in substituent electron-donating ability would be that there is a negligible change in polarity in going from the ground state to the rate-limiting transition state for the reaction. However, it occurred to us that this conclusion might be a result of analyzing our data with a single-parameter linear-free-energy plot. Single-parameter analyses, like the Hammett correlation, have yielded varying amounts of success in interpreting the reactivity in some systems.[39] This is clearly apparent in cases where Hammett plots are nonlinear, but there

(32) Vaughan, G. A.; Hillhouse, G. L.; Rheingold, A. L. *J. Am. Chem. Soc.* **1990**, *112*, 7994.
(33) Polse, J. L.; Andersen, R. A.; Bergman, R. G. *J. Am. Chem. Soc.*, in press.
(34) Cohen, S. A.; Auburn, P. R.; Bercaw, J. E. *J. Am. Chem. Soc.* **1983**, *105*, 1136.
(35) For examples of other structurally characterized Ti diazoalkane complexes see: Kool, L. B.; Rausch, M. D.; Alt, H. G.; Herberhold, M.; Hill, A. F.; Thewalt, U.; Wolf, B. *J. Chem. Soc., Chem. Commun.* **1986**, 408. See also ref 17.
(36) Messerle, L.; Curtis, M. D. *J. Am. Chem. Soc.* **1980**, *102*, 7789.
(37) Curtis, M. D.; Messerle, L.; D'Errico, J. J.; Butler, W. M.; Hay, M. S. *Organometallics* **1986**, *5*, 2283.
(38) Cowie, M.; McKeer, I. R.; Loeb, S. J.; Gauthier, M. D. *Organometallics* **1986**, *5*, 860.
(39) Drago, R. S. *Inorg. Chem.* **1995**, *34*, 3543, and references cited therein.

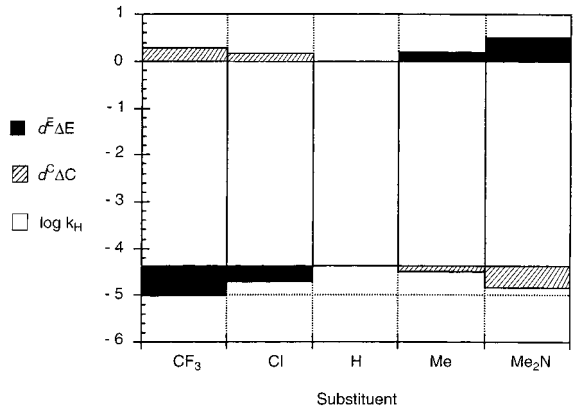

Figure 13. Graphical presentation of eq 3 for the reaction of **5**−**9** with styrene, showing the contribution of electrostatic and covalent effects (relative to **5**) toward the overall rate constant. Adding the three regions for each substituent gives the overall rate constant for that system.

may also be cases in which apparently linear fits disguise more complicated effects of substituents on reaction rates.[40]

To check the conclusion derived from the Hammett analysis, we decided to apply the *E/C* dual parameter substituent mode developed by Drago,[39,41−44] which separates electrostatic from covalent contributions, to our data.[45] The basis for this model is shown in eq 3 and has been described in detail elsewhere.[44]

$$\Delta\chi^X = d^E\Delta E^X + d^C\Delta C^X + \Delta\chi^H \qquad (3)$$

The ΔE^X (electrostatic) and ΔC^X (covalent) constants[44] are the dual parameter analogues of the Hammett substituent constant σ. The parameters d^E and d^C collectively correspond to the Hammett ρ value. The value measured for a substituent X is denoted by $\Delta\chi^X$ (in this case the log of the first-order rate constant). The quality of the fit was excellent (see Supporting Information), and the values obtained for d^E and d^C are 3.6 and −0.53, respectively ($d^E/d^C = -6.8$).

The electrostatic ($d^E\Delta E^X$) and covalent ($d^C\Delta C^X$) contributions of each substituent to the overall rate constant are illustrated graphically in Figure 13. For a given substituent, the electrostatic contribution is shown in black and the covalent contribution is illustrated with hash marks; adding these to the log of the rate constant for X = H gives the overall rate constant. As can be seen from the figure, an interesting dependence emerges. Although the absolute value of $d^E\Delta E^X$ (the electrostatic contribution) is a bit larger in absolute magnitude than the covalent contribution $d^C\Delta C^X$ for all four subsituents, in this reaction the two effects work in opposite directions in each case. The result is that the electrostatic and covalent contributions

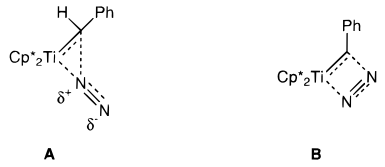

Figure 14.

happen to be the right order of magnitude to make the effect on the rate constant just compensate. If $d^C\Delta C^X$ were either constant or substantially smaller than $d^E\Delta E^X$ for these four substituents, the electrostatic term would have dominated and the Hammett plot would have yielded a steeper slope and a much larger value of ρ. We conclude that the *E*- and *C*-based dual parameter substituent analysis is a useful approach not only when a poor Hammett correlation is obtained but also when the Hammett analysis indicates no effect at all.

There are several possibilities for the structure of the transition state leading to dinitrogen loss. Figure 14 illustrates two of these. One possibility that is often invoked in the reactivity of diazoalkanes to form metal carbene complexes is a transition structure (**A**) in which the diazoalkane is coordinated through the C═N rather than the N═N bond.[46] Another possible structure is **B**. One might have interpreted the Hammett plot to favor structure **B**, since it has less charge separation than **A**. However, the *E/C* analysis suggests that there is a significant electrostatic contribution to the rate, so some charge separation may be occurring in the transition state. Because of the compensating electrostatic and covalent contributions to the transition state, we therefore feel that it is not possible to distinguish between structures **A** and **B** for this reaction.[47]

Lewis Base Induced Coordination Change in 5. Trapping studies of **1** have been reported earlier (Scheme 1).[19] It was found that PMe_3 had no effect on the reaction, and that pyridine or *p*-(dimethylamino)pyridine (DMAP) formed adducts with **1**, but the adducts could not be isolated since the binding was reversible (eq 4).[19] In contrast, Lewis base adduct **16** was

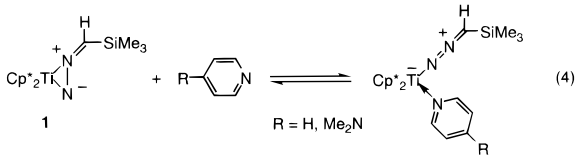

isolated by using ^{t}BuNC (Scheme 3). The product was stable as long as solutions of **16** were not placed under vacuum for extended periods of time. From the spectroscopic data described in the Results, it seems likely that a coordination change of the diazoalkane ligand from η^2 to η^1 occurs. In fact, a similar

(40) The use of multiparameter linear free energy relationships has a long history; see, for example: Lowry, T. H.; Richardson, K. S. *Mechanism and Theory in Organic Chemistry*, 3rd ed.; Harper and Row: New York, 1987; pp 155−159.

(41) Drago, R. S.; Dadmun, A. P. *J. Am. Chem. Soc.* **1994**, *116*, 1792.

(42) Drago, R. S. *Organometallics* **1995**, *14*, 3408.

(43) Drago, R. S. *J. Organomet. Chem.* **1996**, *512*, 61.

(44) Drago, R. S. *Applications of Electrostatic-Covalent Models in Chemistry*; Surfside Scientific: Gainsville, FL, 1994.

(45) There are other approaches to separating substituent effects, including the QALE fits. For leading references see: (a) Wilson, M. R.; Liu, H.; Prock, A.; Giering, W. P. *Organometallics* **1993**, *12*, 2044. (b) Bartholomew, J.; Fernandez, A. L.; Lorsbach, B. A.; Wilson, M. *Organometallics* **1996**, *15*, 295. (c) Fernandez, A.; Reyes, C.; Wilson, M. R.; Woska, D. C.; Prock, A.; Giering, W. P. *Organometallics* **1997**, *16*, 342, and references cited therein. (d) Joerg, S.; Drago, R. S.; Sales, J. *Organometallics* **1998**, *17*, 589, and references cited therein. (e) For another organometallic system to which we have applied this type of analysis, see: Aubart, M. A.; Bergman, R. G. *J. Am. Chem. Soc.* **1998**, *120*, 8755.

(46) Analogous structures have been reported for the isoelectronic ketene metal system. See, for example: (a) Hofmann, P.; Perez-Moya, L. A.; Steigelmann, O.; Riede, J. *Organometallics* **1992**, *11*, 1167. (b) Halfon, S. E.; Fermin, M. C.; Bruno, J. W. *J. Am. Chem. Soc.* **1989**, *111*, 5490. (c) Fermin, M. C.; Bruno, J. W. *J. Am. Chem. Soc.* **1993**, *115*, 7511.

(47) We are grateful for a reviewer's supportive comments about the E/C analysis of the substituent effect data and considered his/her suggestion that the data suggest that **A** is the better model for the transition state structure. However, our argument boils down to the following. The traditional Hammett analysis would lead one to believe that there is little charge separation in the transition state. The *E/C* analysis, on the other hand, suggests that charge separation does exist, but that it is almost exactly compensated for by covalent effects. Therefore, although one transition state is drawn with formal charges, we think it is difficult to predict how much actual overall charge separation there is in **A** vs **B**. We therefore feel that the utility of the *E/C* analysis is to remove the apparent (but misleading) certainty induced by the Hammett analysis—i.e., the *E/C* analysis makes the conclusion more ambiguous than it would otherwise have been. We agree with the reviewer that this is "a bit of a letdown", but we think it is the most honest interpretation of the *E/C* analysis.

Scheme 5

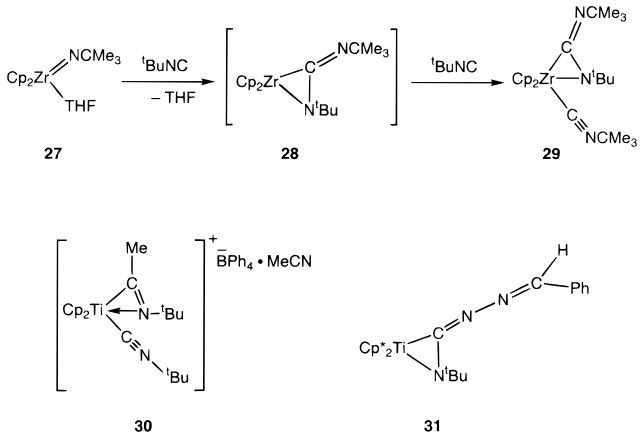

compound $Cp_2Ti(N_2CPh_2)(PMe_3)$ (**26**) has been reported in which the diazoalkane ligand is terminally bound.[17] It seems unlikely that in the bulkier system **16**, the ^{t}BuNC is bound to titanium while the diazoalkane fragment remains η^2-coordinated. Although distinct resonances are observed for the free and coordinated ^{t}BuNC ligand, they do indeed undergo exchange, as demonstrated in an EXSY experiment (Figure 5).

Adduct **16** was observed with 1 or 10 equiv of ^{t}BuNC. In contrast to the systems studied by Walsh et al.[48] or Bochmann et al.,[49] no evidence for the incorporation of more than 1 equiv of ^{t}BuNC into the product was obtained. Both the η^2-carbodiimide isocyanide complex **29** (Scheme 5), formed from the zirconocene imido complex **27** and ^{t}BuNC via intermediate **28**, and the iminoacyl isocyanide complex **30** represent examples of systems in which 2 equiv of isocyanide is incorporated in the coordination sphere; one is terminally bound to the metal center, and the other is inserted into either a metal−carbon bond (**30**) or a metal−nitrogen bond (**29**) (Scheme 5). It is possible that the product formed from reaction of **5** with 1 equiv of ^{t}BuNC is **31** (Scheme 5). However this seems unlikely since the IR spectrum of isolated **16** shows a stretch at 2139 cm^{-1} for the C≡N bond of the isonitrile ligand, and this is too high for the structure illustrated by **31**. In addition, the ready interconversion between bound and free ^{t}BuNC suggests a minor structural rearrangement of the metal fragment, which is also inconsistent with **31**.

^{15}N NMR Study of η^2-Diazoalkane Complex 5 and η^1-Diazoalkane Complex 16. Nitrogen-15 chemical shifts (which can range from +800 to −400 ppm) and coupling constants are sensitive to the disposition of the lone pairs and π electrons.[50] The ^{15}N shifts for the ^{t}BuNC adduct **16** and diazoalkane adduct **5**, as well as their coupling constants to the proton on the diazoalkane ligand, were measured (Figures 5 and 6). For **5**, they are −23.1 ppm (6.3 Hz) and 115.2 ppm (1.5 Hz) relative to nitromethane. For **16**, they are 30 ppm (3.5 Hz) and 132 ppm (2.9 Hz). A likely assignment of the shifts to individual nitrogen atoms is discussed in Results.

Organic diazoalkane complexes have ^{15}N chemical shifts in the range −40 to +60 (terminal) and −30 to −110 (central) ppm relative to nitromethane.[51,52] The nitrogen shifts of PhC(H)N_2 are +83 (terminal) and −56.3 (central) ppm.[51] It seems reasonable that these shifts would change upon coordination to titanium; in fact, most coordination shifts are relatively small, a few tens of parts per million, given the range of the shifts and can vary according to the symmetry of the complex and properties of the metal center (d electron configuration, oxidation, number, and periodicity).[26] Thus, the relatively small coordination shifts in **5** are not surprising. More importantly, however, the shifts for **16** are significantly different from those in **5**, consistent with the postulated change in coordination of the diazoalkane fragment upon adduct formation (vide supra).

Scheme 6

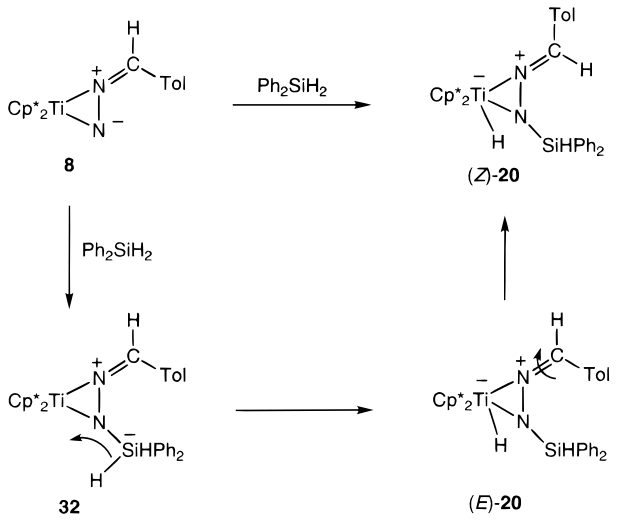

Mechanism of the Reaction of Aryldiazoalkane Complexes with Np_3Al and Silanes. Trineopentylaluminum coordinates to the terminal nitrogen of **8**, indicating that this nitrogen atom is basic (Scheme 3). Silanes add across the Ti−N bond of **8** as shown in Scheme 3. Tilley and co-workers have recently described the addition of silanes to Ta=N double bonds.[53] Addition of silanes to a tantalum-imido complex occurs via initial formation of a Si−N bond, followed by fast intramolecular hydride transfer to the metal center. It is likely that this mechanism is operative in our system as well. A proposed mechanism for the formation of (*Z*)-**20** is outlined in Scheme 6, which is analogous to that proposed by Tilley and co-workers. The first step shown is addition of diphenylsilane to the diazoalkane complex **8** to give intermediate **32**. This undergoes hydride transfer to titanium to yield the *E*-isomer of **20** which was isolated and characterized. Upon standing at room temperature, the *E*-isomer rearranges to (*Z*)-**20** by rotation of the *p*-tolyl group, presumably to alleviate steric congestion.

CO-Induced N−N Bond Fission in 8. As outlined in Results, treatment of **8** with CO affords **21** in good yield (Scheme 3). Relatively few examples exist of similar insertions into metal imido bonds to form isocyanates,[54] despite the fact that this reaction is believed to be involved in the catalytic carbonylation of organoazides and nitroaromatic compounds.[55] Most transition metal-induced N=N bond cleavages have been observed in aromatic diazenes and are relevant to potential nitrogen-fixing transformations.[11,56] Much work has been focused on the interaction of diazenes with titanium complexes.[12]

(48) Walsh, P. J.; Hollander, F. J.; Bergman, R. G. *Organometallics* **1993**, *12*, 3705.
(49) Bochmann, M.; Wilson, L. M.; Hursthouse, M. B.; Short, R. L. *Organometallics* **1987**, *6*, 2556.
(50) Mason, J. *Chem. Br.* **1983**, 654.
(51) Duthaler, R. O.; Förster, H. G.; Roberts, J. D. *J. Am. Chem. Soc.* **1978**, *100*, 4974.
(52) Blumenfeld, A. L.; Lenenko, V. C.; Lorentz, B.; Mobius, I.; Wahren, M.; Shur, W. B.; Volpin, M. E. *Dokl. Akad. Nauk SSSR* **1980**, *251*, 611.
(53) Gountchev, T. I.; Tilley, T. D. *J. Am. Chem. Soc.* **1997**, *119*, 12831.
(54) Rosen, R. Ph.D. Dissertation, University of California at Berkeley, 1989.
(55) La Monica, G.; Cenini, S. *J. Organomet. Chem.* **1981**, *216*, C35.
(56) Mastropasqua, P.; Riemer, A.; Kisch, H. *J. Organomet. Chem.* **1978**, *148*, C40.

Scheme 7

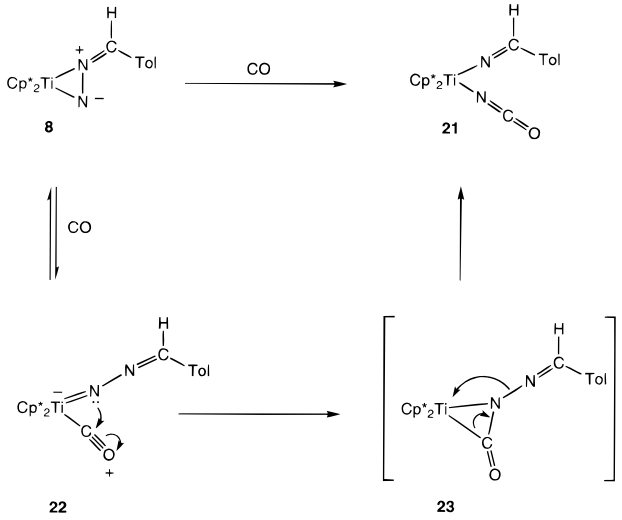

This is due in part to the importance of titanium species in organic synthesis.[57] Some N−N bond cleavage reactions to form isocyanato ligands have also been documented for metal hydrazido complexes.[58]

The reaction of diazoalkane complex **8** with CO to form **21** represents an unusual example of diazoalkane N−N bond cleavage at a monomeric metal center. The related cleavage of the CO bond of a coordinated ketene ligand by isocyanide has been described[59] and differs from the reactivity of a coordinated diazoalkane ligand toward isocyanide, as described in Results. This transformation may be relevant to the chemistry of nitrogen fixation. It has been shown that Mo and W systems can coordinate dinitrogen and that the dinitrogen ligands may be converted to diazoalkane ligands.[3,11] We have shown that a diazoalkane adduct may then be treated with CO to cleave the N−N bond. There are also several notable examples of multinuclear complexes which undergo N−N bond fission at a bridging diazoalkane ligand.[3]

A possible mechanistic pathway for the formation of **21** is shown in Scheme 7. The first step, similar to the reaction of **5** with ^{t}BuNC (vide supra), involves coordination of CO to the titanium center and a coordination change from η^2 to η^1 for the diazoalkane complex to form intermediate **22**. As discussed in Results, this species is observed by ^{1}H NMR, but attempts to isolate **22** by removing the solvent resulted in the regeneration of **8**. We propose complex **22** is further transformed by attack of the titanium bound nitrogen on the bound CO carbon to form **23**.[60,61] Cleavage of the Ti−C bond in **23** and cleavage of the N−N bond to form a Ti−N bond gives the observed product **21**.

Summary

We have synthesized and characterized several aryldiazoalkane complexes of titanium (**5**−**10**) from $Cp^*_2Ti(C_2H_4)$ (**4**) and organic diazoalkanes and have shown that in the solid state these complexes have η^2-N_2-diazoalkane ligands. Unlike the majority of previously known diazoalkane complexes, **5**−**9** release dinitrogen in solution at 75 °C, and the resulting carbene fragments can be trapped by an olefin. A Hammett σ/ρ study designed to investigate the distribution in charge in the rate-determining transition state gave almost no dependence of the rate on changing substituents, suggesting that there is little change in charge separation in going to the transition state. However, application of the *E*- and *C*-based dual parameter substituent constant analysis showed that the electrostatic and covalent contributions of each substituent to the reaction rate almost exactly cancel, resulting in the very low value of ρ in the Hammett correlation.

The increased thermal stability of **5**−**9** has also allowed us to study the reaction chemistry of these complexes, which have demonstrated several different modes of reactivity: (1) loss of dinitrogen to form transient carbene complexes; (2) coordination change of the diazoalkane ligand from η^2 to η^1 upon addition of Lewis base; (3) Lewis acid coordination to the terminal nitrogen; (4) addition of silanes across the Ti−N bond; (5) cleavage of the N−N bond by CO.

Experimental Section

General Methods. Unless otherwise noted, all reactions and manipulations were carried out in dry glassware under a nitrogen or argon atmosphere at 20 °C in a Vacuum Atmospheres 553-2 drybox equipped with a MO-40-2 inert gas purifier or using standard Schlenk techniques. The amount of O_2 in the drybox atmosphere was monitored with a Teledyne Model No. 316 trace oxygen analyzer. Some reactions were carried out in thick-walled glass vessels fused to vacuum stopcocks; these are referred to in the procedures as glass bombs. The other instrumentation and general procedures used have been described previously.[62]

Unless otherwise specified, all reagents were purchased from commercial suppliers and used without further purification. Dimethyoxybenzene was sublimed prior to use. Styrene was stirred over activated 4 Å molecular sieves, vacuum distilled, and then stored at −50 °C in contact with activated 4 Å molecular sieves. Acetylene gas was purified by passage through two −78 °C traps separated by a concentrated H_2SO_4 trap. $Cp^*_2Ti(C_2H_4)$ was prepared by the literature method,[34] except that Cp^*_2TiCl[63] was used instead of $Cp^*_2TiCl_2$. Np_3Al was prepared by the literature method.[64] The monoaryl diazoalkanes were prepared by the method of Closs and Moss,[65] isolated as solutions, and dried over activated 4 Å molecular sieves at 0 °C for 3 h prior to titration with diphenylacetic acid and use. Ph_2CN_2 was prepared by the literature method.[66] For analogous complexes, elemental analyses were performed only on select representative materials.

NMR Spectroscopy. NMR experiments were performed on a Brucker AMX spectrometer resonating at 300.13 MHz for ^{1}H and 75.42 MHz for ^{13}C that was equipped with an inverse probe. One-dimensional $^{13}C\{^1H\}$ spectra and DEPT spectra were recorded on a Brucker AMX spectrometer resonating at 400 MHz for ^{1}H and 100 MHz for ^{13}C that was equipped with a QNP probe. All two-dimensional experiments were acquired between 295 and 300 K. NOESY spectra were acquired in phase-sensitive mode using the Brucker pulse program noesytp. A shifted sine-bell window function was applied to the raw data set in both dimensions. $^1H-^{15}N$ correlation spectra were recorded on a Bruker DMX 600 at 298 K unless otherwise stated. Final $^1H-^{15}N$ correlation spectra were recorded using a modified fast HSQC sequence[28] employing triple axis gradients without refocusing and decoupling. In a typical experiment used for $Cp^*_2Ti(N_2CHPH)(^t$BuNC) (**16**), 256 t_1 points over a spectral width of 600 ppm were collected in F_1. The

(57) Hegedus, L. S. *Transition Metals in the Synthesis of Complex Organic Molecules*; University Science Books: Mill Valley, CA, 1994.
(58) Walsh, P. J.; Carney, M. J.; Bergman, R. G. *J. Am. Chem. Soc.* **1991**, *113*, 6333.
(59) Fermin, M. C.; Bruno, J. W. *J. Am. Chem. Soc.* **1993**, *115*, 7511.
(60) A similar intermediate was proposed for the reaction of $Cp_2Ti(CO)_2$ with diphenyldiazomethane. See ref 17.
(61) A possible alternative mechanism would involve a coordination change of the diazoalkane ligand in the CO adduct from η^1 to η^2. This would cause steric congestion but would create a more nucleophilic nitrogen atom. We thank a reviewer for this suggestion.
(62) Meyer, K. E.; Walsh, P. J.; Bergman, R. G. *J. Am. Chem. Soc.* **1995**, *117*, 3749.
(63) Pattiasina, J. W.; Heeres, H. J.; Bolhuis, F. v.; Meetsma, A.; Teuben, J. H. *Organometallics* **1987**, *6*, 1004.
(64) Beachley, O. T., Jr.; Victoriano, L. *Organometallics* **1988**, *7*, 63.
(65) Closs, G. L.; Moss, R. A. *J. Am. Chem. Soc.* **1964**, *86*, 4042.
(66) Miller, J. B. *J. Org. Chem.* **1959**, *24*, 560.

acquisition time in t_2 was 0.36 s, 160 scans per increment being collected. Gradients were sine shaped, 2 ms duration, and up to ca. 20 G/cm in strength. Delays were optimized for couplings of 6 Hz. Proton shifts were recorded relative to C_6D_5H at 7.15 ppm. ^{15}N shifts were referenced to hypothetical nitromethane by using $\Xi = 10.136\,783$ relative to the proton 0 ppm frequency.[67] Coupling constants were measured or estimated from the antiphase splittings using an 8-fold J multiplication procedure from spectra which were zero filled to better than 0.2 Hz/data point.[68] Gradient enhanced HMBC experiments with a wider F_1 spectral range and ^{15}N pulses < 90° were recorded prior to the fast HSQC experiments to ensure that no folding took place.

Cp*$_2$Ti(N$_2$C(H)C$_6$H$_5$) (5). Phenyldiazomethane (72 mL of a 0.02 M solution in benzene, 1.39 mmol) was added dropwise to a stirred solution of **4** (482 mg, 1.39 mmol) in toluene (15 mL). Gas evolution ensued and the solution turned from lime green to forest green within 30 s. The solution was stirred for 10 min, and the volatile materials were removed under vacuum. The dark green powder was washed with hexanes (10 mL), dissolved in toluene (15 mL), and cooled to −50 °C to yield **5** as green crystals (447 mg, 75%). ^1H NMR (C_6D_6): δ 7.89 (d, J = 7.7 Hz, 2 H), 7.36 (t, J = 7.4 Hz, 2 H), 6.99 (t, J = 7.5 Hz, 1 H), 5.45 (s, 1 H), 1.65 (s, 30 H) ppm. $^{13}C\{^1H\}$ (C_6D_6): δ 138.1 (C), 128.6 (CH), 126.9 (CH), 123.9 (CH), 122.5 (C), 107.4 (CH), 11.2 (CH_3) ppm. ^{15}N (C_6D_6): δ −23.1 (J_{NH} = 6.26 Hz), 115.2 (J_{NH} = 1.5 Hz) ppm. IR (Nujol): 1591 (m), 1579 (w), 1491 (s), 1448 (s), 1327 (m), 1302 (w), 1286 (m), 1273 (w), 1261 (w), 1209 (w), 1173 (w), 1167 (w), 1153 (w), 1117 (w), 1088 (m), 1065 (m), 1020 (m), 989 (w), 752 (m), 690 (m), 546 (s), 505 (s) cm^{-1}. MS-EI: m/z = 436 [M$^+$]. HRMS (EI) for $C_{27}H_{36}N_2Ti$: m/z(calcd) = 436.2358; m/z(obsd) = 436.2355.

Cp*$_2$Ti(N$_2$C(H)C$_6$H$_4$CF$_3$) (6). Using the procedure for **5**, 26 mL of (*p*-(trifluoromethyl)phenyl)diazomethane (0.04 M solution in hexanes, 1.04 mmol), 360 mg of **4** (0.104 mmol), and 331 mg (63%) of **6** were obtained. ^1H NMR (C_6D_6): δ 7.75 (br, 2 H), 7.56 (d, J = 8.5 Hz, 2 H), 5.34 (s, 1 H), 1.59 (s, 30 H) ppm. $^{13}C\{^1H\}$ (C_6D_6; CF_3 carbon and adjacent ring carbon were not observed): δ 140.7 (C), 125.7 (q, J = 3.8 Hz, CH), 123.1 (C), 122.8 (CH), 105.8 (CH), 11.1 (CH_3) ppm. $^{19}F\{^1H\}$ (C_6D_6): δ −61.4 ppm. IR (Nujol): 1599 (s), 1556 (m), 1508 (s), 1498 (s), 1421 (s), 1394 (s), 1323 (s), 1219 (m), 1176 (s), 1118 (s), 1049 (s), 1018 (s), 953 (w), 858 (m), 843 (s), 831 (s), 804 (w), 789 (m), 737 (m), 715 (m), 598 (m) cm^{-1}; MS-EI: m/z = 504 [M$^+$]. Anal. Calcd for $C_{28}H_{35}N_2F_3Ti$: C, 66.66; H, 6.99; N, 5.55. Found: C, 66.64; H, 7.18; N, 5.33.

Cp*$_2$Ti(N$_2$C(H)C$_6$H$_4$Cl) (7). Using the procedure for **5**, 15.6 mL of (*p*-chlorophenyl)diazomethane (0.07 M solution in pentane, 0.109 mmol) and 379 mg of **4** (1.09 mmol), 347 mg (67%) of **7** was obtained. ^1H NMR (C_6D_6): δ 7.66 (br d, J = 8.0 Hz, 2 H), 7.30 (d, J = 8.8 Hz, 2 H), 5.32 (s, 1 H), 1.62 (s, 30 H) ppm. $^{13}C\{^1H\}$ (C_6D_6): δ 136.5 (C), 128.7 (CH), 127.1 (C), 124.8 (CH), 122.7 (C), 106.2 (CH), 11.2 (CH_3) ppm. IR (Nujol): 1572 (m), 1564 (m), 1483 (s), 1441 (s), 1363 (s), 1325 (m), 1174 (m), 1086 (m), 1068 (s), 1041 (s), 816 (m), 723 (m), 559 (m) cm^{-1}. MS-EI: m/z = 470 [M$^+$].

Cp*$_2$Ti(N$_2$C(H)C$_6$H$_4$Me) (8). *p*-Tolyldiazomethane (17 mL of a 0.15 M solution in pentane, 2.96 mmol) was added dropwise to a stirred solution of **4** (1.024 g, 2.96 mmol) in C_6H_6 (40 mL). Gas evolution ensued, and the solution turned from lime green to forest green within 1 min. The solution was stirred for 30 min, and the volatile materials were removed under vacuum. The dark green powder was dissolved in toluene (20 mL) and cooled to −50 °C to yield **8** as green crystals (710 mg, 64.7%). ^1H NMR (C_6D_6): δ 7.83 (d, J = 8.1 Hz, 2 H), 7.17 (d, J = 8.1 Hz, 2 H), 5.46 (s, 1 H), 2.19 (s, 3 H), 1.67 (s, 30 H) ppm. $^{13}C\{^1H\}$ (C_6D_6): δ 134.7 (C), 130.7 (C), 127.3 (CH), 123.2 (CH), 121.5 (C), 106.9 (CH), 20.3 (CH_3), 10.3 (CH_3) ppm. IR (Nujol): 1581 (m), 1512 (s), 1493 (s), 1481 (s), 1468 (s), 1454 (s), 1441 (s), 1431 (s), 1421 (s), 1404 (s), 1387 (s), 1365 (s), 1352 (s), 1342 (s), 1313 (m), 1300 (m), 1221 (m), 1211 (m), 1030 (s), 804 (m), 712 (m), 523 (s), 501 (s) cm^{-1}. MS-EI: m/z = 450 [M$^+$]. Anal. Calcd for $C_{28}H_{38}N_2Ti$: C, 74.65; H, 8.50; N, 6.22. Found: C 74.43; H, 8.65; N, 6.11.

Cp*$_2$Ti(N$_2$C(H)C$_6$H$_4$NMe$_2$) (9). Using the procedure for **5**, 75 mL of (*p*-(dimethylamino)phenyl)diazomethane (0.008 M solution in pentane, 0.640 mmol), 389 mg of **4** (1.12 mmol), and 199 mg (37%) of **9** were obtained. ^1H NMR (C_6D_6): δ 7.87 (d, J = 8.9 Hz, 2 H), 6.80 (d, J = 8.9 Hz, 2 H), 5.53 (s, 1 H), 2.56 (s, 6 H), 1.72 (s, 30 H) ppm. $^{13}C\{^1H\}$ (C_6D_6): δ 147.5 (C), 128.6 (C), 125.5 (CH), 122.0 (C), 114.0 (CH), 108.8 (CH), 40.8 (CH_3), 11.3 (CH_3) ppm. IR (Nujol): 1605 (m), 1470 (s), 1444 (s), 1383 (s), 1311 (s), 1219 (m), 1167 (m), 1066 (m), 1024 (m), 947 (m), 812 (s), 727 (w), 553 (m) cm^{-1}. MS-EI: m/z = 479 [M$^+$].

Cp*$_2$Ti(N$_2$CPh$_2$) (10). A solution of diphenyldiazomethane (66.1 mg, 0.340 mmol) in C_6H_6 (4 mL) was added dropwise to a stirred solution of **4** (118 mg, 0.340 mmol) in C_6H_6 (8 mL). Gas evolution ensued, and the solution turned from lime green to brown within 30 s. The solution was stirred for 10 min, and the volatile materials were removed under vacuum. The brown powder was washed with hexanes (10 mL), dissolved in toluene (10 mL), and cooled to −50 °C to yield **10** as a green microcrystalline solid (90 mg, 65%). ^1H NMR (C_6D_6): δ 8.11 (d, J = 7.2 Hz, 2 H), 7.32 (t, J = 7.8 Hz, 2 H), 7.07 (t, J = 7.3 Hz, 1 H), 6.96 (t, J = 7.4 Hz, 2 H), 6.86 (t, J = 2.1 Hz, 1 H), 6.29 (d, J = 7.3 Hz, 2 H), 1.67 (s, 30 H) ppm. $^{13}C\{^1H\}$ (C_6D_6): δ 139.0 (C), 138.8 (C), 128.1 (CH), 127.7 (CH), 127.5 (CH), 124.8 (CH), 124.1 (CH), 123.4 (C), 122.2 (CH), 114.7 (C), 11.4 (CH_3) ppm. The shifts of overlapping ^{13}C resonances were determined by HMQC;[21] the spectrum is included in the Supporting Information. IR (Nujol): 3062 (w), 1593 (m), 1487 (s), 1429 (s), 1333 (m), 1309 (w), 1279 (w), 1263 (w), 1232 (w), 1173 (w), 1147 (w), 1111 (m), 1093 (w), 1082 (w), 1068 (w), 1024 (m), 951 (w), 760 (w), 739 (w), 696 (m), 673 (w), 667 (m), 622 (w), 613 (w) cm^{-1}. MS-EI: m/z = 512 [M$^+$]. HRMS (EI): for $C_{33}H_{41}N_2Ti$: m/z(calcd) = 513.2749 [MH$^+$]; m/z(obsd) = 513.2759. Anal. Calcd for $C_{33}H_{40}N_2Ti$: C, 77.33; H, 7.87; N, 5.47. Found: C, 77.41; H, 7.54; N, 5.63.

Cp*$_2$Ti(CHPhCHPhCH$_2$) (11). Styrene (825 mg, 7.92 mmol) was added to a solution of **5** (346 mg, 0.792 mmol) in C_6H_6 (10 mL). The solution was heated to 75 °C in a bomb for 26 h, and the volatile materials were removed under vacuum. The resulting brown powder was washed with ether (7 × 0.5 mL), dissolved in toluene (8 mL), and cooled to −50 °C to yield **11** as red crystals (256 mg, 63%). ^1H NMR (C_6D_6): δ 7.47 (d, J = 7.5, 2 H, *o*-Ph), 7.24 (t, J = 7.5, 2 H, *m*-Ph), 7.09 (t, J = 7.3, 1 H, *p*-Ph), 7.01 (t, J = 7.6, 2 H, *m*-Ph), 6.90 (t, J = 7.0, 1 H, *p*-Ph), 6.67 (d, J = 7.6, 2 H, *o*-Ph), 3.72 (d, J = 10.9, 1 H), 1.88 (m, 1 H), 1.83 (m, 1 H), 1.77 (s, 15 H), 1.70 (m, 1 H), 1.53 (s, 15 H) ppm. $^{13}C\{^1H\}$ NMR (C_6D_6): δ 151.3 (C), 147.6 (C), 129.1 (CH), 128.5 (CH), 127.9 (CH), 126.9 (CH), 125.0 (CH), 122.3 (CH), 120.8 (C), 120.2 (C), 76.8 (CH_2), 67.9 (CH), 24.1 (CH), 12.7 (CH_3), 11.8 (CH_3) ppm. IR (C_6H_6): 2963 (w), 2945 (w), 2913 (m), 2903 (m), 2894 (m), 2856 (m), 2292 (w), 1633 (w), 1593 (m), 1442 (m), 1410 (w), 1379 (m), 1218 (w), 1197 (w), 1076 (w), 1065 (w), 746 (m), 700 (m) cm^{-1}. MS-EI: m/z = 513 [M$^+$]. Anal. Calcd for $C_{35}H_{44}Ti$: C, 82.01; H, 8.65. Found: C, 82.52; H, 8.65.

Cp*$_2$Ti(CH(C$_6$H$_4$CF$_3$)CHPhCH$_2$) (12). Styrene (302 mg, 2.90 mmol) was added to a solution of **6** (146 mg, 0.290 mmol) in C_6H_6 (10 mL). The solution was heated to 75 °C in a bomb for 35.5 h, and the volatile materials were removed under vacuum. The resulting brown powder was washed with ether (3 × 1 mL), dissolved in ether (12 mL), and cooled to −50 °C to yield **12** as red crystals (97.6 mg, 58%). ^1H NMR (C_6D_6): δ 7.36 (d, J = 7.5, 2 H), 7.23 (t, J = 7.9, 3 H), 7.10 (d, J = 7.4, 2 H), 6.55 (d, J = 8.2, 2 H), 3.60 (d, J = 9.5, 1 H), 1.79 (m, 1 H), 1.75 (m, 1 H), 1.72 (s, 15 H), 1.61 (m, 1 H), 1.44 (s, 15 H) ppm. $^{13}C\{^1H\}$ NMR (C_6D_6; CF_3 carbon and adjacent carbon were not observed): δ 156.4 (C), 146.7 (C), 129.7 (CH), 128.9 (CH), 128.0 (CH), 125.3 (CH), 123.7 (CH), 121.2 (C), 120.4 (C), 76.5 (CH_2), 65.4 (CH), 24.0 (CH), 12.7 (CH_3), 11.7 (CH_3) ppm. $^{19}F\{^1H\}$ NMR (C_6D_6): δ −61.3 ppm. IR (Nujol): 3090 (m), 3072 (m), 3033 (s), 2903 (w), 2874 (w), 1960 (w), 1815 (w), 1607 (w), 1479 (m), 1325 (m), 1160 (w), 1115 (w), 1067 (w), 1035 (m), 681 (s), 663 (m) cm^{-1}. MS-EI: m/z = 581 [M$^+$]. Anal. Calcd for $C_{35}H_{44}Ti$: C, 74.47; H, 7.46. Found: C, 74.18; H, 7.64.

Cp*$_2$Ti(CH(C$_6$H$_4$Cl)CHPhCH$_2$) (13). Styrene (456 μL, 3.98 mmol) was added to a solution of **7** (187 mg, 0.398 mmol) in C_6H_6 (10 mL). The solution was heated to 75 °C in a bomb for 35.5 h. The solution

(67) Harris, R. K. *Nuclear Magnetic Resonance Spectroscopy, a Physiochemical View*; Pitman: Marshfield, MA, 1983; p 230.

(68) Delrioportilla, F.; Blechta, V.; Freeman, R. *J. Magn. Reson., A* **1994**, *111*, 132.

was cooled to room temperature, and the volatile materials were removed under vacuum. The resulting brown powder was washed with ether (5 × 1 mL), dissolved in ether (12 mL), and cooled to −50 °C to yield **13** as red crystals (111 mg, 51%). ^{1}H NMR (C_6D_6): δ 7.39 (d, J = 7.5, 2 H, *o*-Ph), 7.24 (t, J = 7.6, 2 H, *m*-Ph), 7.11 (t, J = 7.6, 1 H, *p*-Ph), 6.96 (d, J = 8.5, 2 H), 6.45 (d, J = 8.5, 2 H), 3.53 (d, J = 11.0, 1 H), 1.82 (m, 1 H), 1.78 (m, 1 H), 1.72 (s, 15 H), 1.62 (m, 1 H), 1.47 (s, 15 H) ppm. ^{13}C{^{1}H} NMR (C_6D_6): δ 150.0 (C), 147.0 (C), 129.5 (CH), 129.3 (C), 129.0 (CH), 128.2 (CH), 126.9 (CH), 125.2 (CH), 120.9 (C), 120.2 (C), 76.5 (CH_2), 67.0 (CH), 24.1 (CH), 12.7 (CH_3), 11.7 (CH_3) ppm. IR (Nujol): 3088 (m), 3071 (m), 3034 (s), 2956 (w), 2910 (w), 1959 (w), 1815 (w), 1594 (w), 1584 (w), 1480 (m), 1452 (w), 1378 (w), 1193 (w), 1091 (w), 1053 (m), 814 (w), 715 (w), 700 (m), 681 (s), 666 (s) cm^{-1}. MS-EI: m/z = 547 [M$^+$].

$Cp^*_2Ti(CH(C_6H_4Me)CHPhCH_2)$ (14). Styrene (1.404 g, 13.5 mmol) was added to a solution of **8** (500 mg, 1.35 mmol) in C_6H_6 (25 mL). The solution was heated to 75 °C in a bomb for 30 h, and the volatile materials were removed under vacuum. The resulting red-brown powder was washed with ether (3 × 0.5 mL), dissolved in ether (7 mL), and cooled to −50 °C to yield **14** as red crystals (410 mg, 55%). ^{1}H NMR (C_6D_6): δ 7.49 (d, J = 7.7, 2 H), 7.25 (t, J = 7.7, 2 H), 7.10 (t, J = 7.5, 1 H), 6.85 (d, J = 8.0, 2 H), 6.60 (d, J = 8.0, 2 H), 3.70 (d, J = 10.8, 1 H), 2.19 (s, 3 H), 1.84 (m, 1 H), 1.83 (m, 1 H), 1.79 (s, 15 H), 1.71 (m, 1 H), 1.56 (s, 15 H) ppm. ^{13}C{^{1}H} NMR (C_6D_6): δ 148.1 (C), 147.8 (C), 131.0 (C), 129.2 (CH), 128.4 (CH), 128.2 (CH), 127.6 (CH), 125.0 (CH), 120.7 (C), 120.1 (C), 76.8 (CH_2), 68.3 (CH), 24.1 (CH), 21.0 (CH_3), 12.7 (CH_3), 11.8 (CH_3) ppm. IR (C_6H_6): 3011 (m), 2997 (m), 2956 (m), 2918 (m), 2907 (m), 2874 (m), 1605 (w), 1594 (w), 1506 (m), 1444 (m), 1378 (m), 1222 (w), 1196 (w), 1019 (w), 808 (m), 740 (m), 700 (m), 675 (m), 607 (w), 527 (w) cm^{-1}. MS-EI: m/z = 526 [M$^+$].

$Cp^*_2Ti(CH(C_6H_4NMe_2)CHPhCH_2)$ (15). Styrene (0.651 mg, 6.26 mmol) was added to a solution of **9** (300 mg, 0.626 mmol) in C_6H_6 (10 mL). The solution was heated in a bomb for 26 h, and the volatile materials were removed under vacuum. The resulting brown powder was washed with ether (0.5 mL), dissolved in ether (4 mL), and cooled to −50 °C to yield **15** as red crystals (160 mg, 46%). ^{1}H NMR (C_6D_6): δ 7.52 (d, J = 7.5, 2 H), 7.28 (d, J = 7.5, 2 H), 7.04 (m, 3 H), 6.57 (d, J = 7.5, 2 H), 3.70 (d, J = 11.2, 1 H), 2.12 (m, 1 H), 1.83 (s, 15 H),1.76 (m, 1 H), 1.72 (m, 1 H) 1.59 (s, 15 H) ppm. ^{13}C{^{1}H} NMR (C_6D_6): δ 148.1 (C), 147.5 (C), 140.1 (C), 129.0 (CH), 128.8 (CH), 128.5 (CH), 128.1 (CH), 128.0 (CH), 120.5 (C), 12.0 (C), 77.0 (CH_2), 69.0 (CH), 40.9 (CH_3), 24.2 (CH), 12.5 (CH_3), 11.6 (CH_3) ppm. IR (Nujol): 3016 (m), 2998 (m), 2954 (m), 2910 (m), 2873 (m), 1585 (w), 1500 (m), 1430 (m), 1378 (m), 1233 (w), 1021 (w), 808 (m), 752 (w), 699 (m), 675 (m), 502 (w) cm^{-1}. MS-EI: m/z = 556 [M$^+$].

Kinetic Studies. Kinetics were carried out in 5 mm NMR tubes placed in a constant-temperature bath set at 78.0 ± 0.1 °C. Times of thermolyses were monitored using a digital stopwatch. Upon removal of the thermolyzed samples from the kinetic bath, the temperature of the samples was lowered quickly by placing them immediately in a flask of dry ice/2-propanol. A typical sample preparation and run for the formation of **14** from **8** and styrene are described below. An oven-dried 1 mL volumetric flask was charged with dimethoxybenzene (5.0 mg, 0.036 mmol) and crystals of **8** (13.0 mg, 0.029 mmol). The total volume was brought to 1 mL with toluene-d_8. To an oven-dried J-Young NMR tube was transferred 0.5 mL of the stock solution, followed by 30 μL (0.26 mmol) of styrene. An initial ^{1}H NMR spectrum of the sample was taken. To avoid any complications due to different relaxation times for the various resonances, spectra were recorded using one $\pi/2$ pulse. The samples were allowed to equilibrate in the spectrometer for at least 2 min prior to acquiring the FID. The sample was heated at 78.0 °C for recorded amounts of time; NMR spectra at each time period were recorded. An automatic base-line correction was applied to the data. Integrals were placed manually but not phased. Absolute concentrations of each reagent were determined on the basis of integration relative to the dimethoxybenzene resonance.

$Cp^*_2Ti(N_2C(H)C_6H_5)(CN^tBu)$ (16). To a solution of **5** (223 mg, 0.511 mmol) in toluene (8 mL) was added ^{t}BuNC (43 mg, 0.511 mmol). The solution was stirred 15 min at room temperature, during which time the solution turned from green to red. The solution was concentrated to 3 mL in vacuo and cooled to −50 °C to yield **16** as red crystals (191 mg, 72%). ^{1}H NMR (C_6D_6): δ 7.60 (d, J = 7.7, 1 H), 7.28 (t, J = 7.6, 2 H), 6.91 (t, J = 7.1, 2 H), 6.48 (s, 1 H), 1.88 (s, 30 H), 1.14 (s, 9 H) ppm. ^{13}C{^{1}H} (C_6D_6): δ 170.5 (C), 141.8 (C), 128.7 (CH), 128.4 (CH), 122.3 (CH), 121.2 (CH), 114.1 (C), 56.5 (C), 30.4 (CH_3), 12.0 (CH_3) ppm. ^{15}N (C_6D_6): δ 30 (J_{NH} = 3.5 Hz), 132 (J_{NH} = 2.9 Hz) ppm. IR (C_6H_6): 2608 (w), 2139 (s), 1593 (m), 1494 (m), 1477 (s), 1461 (m), 1418 (m), 1382 (s), 1370 (s), 1320 (w), 1203 (w), 1183 (w), 1159 (m), 1068 (w), 1053 (m), 1024 (w), 992 (w) cm^{-1}. Anal. Calcd for $C_{32}H_{45}N_3Ti$: C, 73.97; H, 8.73; N, 8.09. Found: C 74.32; H, 8.78; N, 7.97.

$Cp^*_2TiN(AlNp_3)N(C(H)C_6H_4Me)$ (17). To a solution of **8** (258 mg, 0.573 mmol) in C_6H_6 (20 mL) was added Np_3Al (138 mg, 0.573 mmol). The solution was stirred for 1 day at room temperature, during which time the solution turned from green to red. The volatile materials were removed under vacuum, and the red powder was washed with hexanes (10 mL), dissolved in toluene (15 mL), and cooled to −50 °C to yield **17** as red crystals (245 mg, 62%). ^{1}H NMR (C_6D_6): δ 7.80 (s, 1 H), 6.79 (d, J = 7.7, 2 H), 6.24 (d, J = 7.7, 2 H), 2.10 (s, 3 H), 1.76 (s, 30 H), 1.67 (s), 0.41 (s) ppm. ^{13}C{^{1}H} NMR (C_6D_6): δ 134.4 (C), 132.7 (C), 129.1 (CH), 128.1 (CH), 122.4 (C), 119.6 (CH), 36.0 (CH_3), 33.3 (C), 20.7 (CH_2), 12.6 (CH_3), 10.9 (CH_3) ppm. IR (Pentane): 2774 (w), 1519 (m), 1483 (w), 1460 (w), 1438 (w), 1410 (w), 1379 (m), 1356 (w), 1218 (w), 1119 (m), 1100 (m), 1011 (w), 826 (w), 633 (w), 582 (w) cm^{-1}. Anal. Calcd for $C_{43}H_{71}AlN_2Ti$: C, 74.75; H, 10.36; N, 4.05. Found: C, 74.81; H, 10.25; N, 4.17.

(*Z*)-$Cp^*_2Ti(H)(N(SiH_2Ph)(N{=}C(H)C_6H_4Me)$ ((*Z*)-19). To a solution of **8** (327 mg, 0.726 mmol) in C_6H_6 (17 mL) was added $PhSiH_3$ (95.0 mg, 0.882 mmol). The solution was stirred for 2 days at room temperature, during which time it turned from green to yellow-orange. The volatile materials were removed under vacuum, and the orange powder was washed with $(Me_3Si)_2O$ (0.5 mL), dissolved in ether (1.5 mL), and cooled to −50 °C to yield (*Z*)-**19** as yellow crystals (315 mg, 78%). ^{1}H NMR (C_6D_6): δ 8.06 (s, 1 H), 7.96 (d, J = 7.8, 2 H), 7.44 (d, J = 8.1, 2 H), 7.24 (m, 3 H), 7.01 (d, J = 7.8, 2 H), 5.63 (s, J_{HSi} = 207.8, 2 H), 3.54 (s, 1 H), 2.15 (s, 3 H), 1.83 (s, 30 H) ppm. ^{13}C{^{1}H} NMR (C_6D_6): δ 137.1 (C), 136.1 (CH), 135.4 (C), 133.6 (CH), 132.9 (C), 130.2 (CH), 129.1 (CH), 128.4 (CH), 126.2 (CH), 114.9 (C), 21.4 (CH_3), 12.8 (CH_3) ppm. IR (pentane): 2168 (w), 2097 (m), 1534 (m), 1509 (w), 1468 (w), 1448 (w), 1429 (m), 1374 (m), 1254 (m), 1231 (w), 1146 (m), 1110 (m), 1059 (m), 1023 (w), 913 (w), 888 (m), 865 (s), 809 (m), 699 (m), 639 (m) cm^{-1}. MS-EI: m/z = 557 [M$^+$ − 1]. Anal. Calcd for $C_{34}H_{46}N_2SiTi$: C, 73.09; H, 8.03; N, 5.01. Found: C, 72.88; H, 8.04; N, 4.88.

(*E*)-$Cp^*_2Ti(H)(N(SiH_2Ph)(N{=}C(H)C_6H_4Me)$ ((*E*)-19). ^{1}H NMR (C_6D_6): δ 7.40 (s, 1 H), 7.25 (m), 7.23 (m), 7.11 (m), 7.03 (m), 5.52 (s, SiH_2, 2 H), 3.36 (s, Ti−*H*, 1 H), 2.11 (s, $C_6H_4CH_3$, 3 H), 1.82 (s, Cp*, 30 H) ppm.

(*E*)-$Cp^*_2Ti(H)(N(SiHPh_2)(N{=}C(H)C_6H_4Me)$ ((*E*)-20). To a solution of **8** (75 mg, 0.117 mmol) in C_6H_6 (15 mL) was added Ph_2SiH_2 (31 mg, 0.117 mmol). The solution was stirred for 36 h at room temperature, during which time the solution turned from dark green to olive green. The volatile materials were removed under vacuum, and the olive green powder was dissolved in ether (0.5 mL) and cooled to −50 °C to yield (*E*)-**20** as yellow-green crystals (57 mg, 54%). ^{1}H NMR (C_6D_6): δ 7.66 (m, 4 H), 7.40 (s, 1 H), 7.36 (d, J = 7.7, 2 H), 7.12 (m, 6 H), 6.97 (d, J = 7.7, 2 H), 6.14 (s, J_{HSi} = 206.9, 1 H), 3.70 (s, 1 H), 2.13 (s, 3 H), 1.80 (s, 30 H) ppm. ^{13}C{^{1}H} (C_6D_6): δ 138.2 (C), 138.1 (C), 136.2 (CH), 133.0 (C), 131.4 (CH), 130.1 (CH), 129.0 (CH), 127.3 (CH), 124.1 (CH), 113.7 (C), 21.3 (CH_3), 12.4 (CH_3) ppm. IR (C_6H_6): 2884 (w), 2975 (w), 2957 (w), 2937 (w), 2903 (m), 2851 (w), 2140 (w), 2094 (m), 1609 (w), 1532 (w), 1509 (w), 1428 (m), 1376 (m), 1108 (m), 1075 (w), 1065 (w), 970 (s), 870 (m), 842 (m), 812 (m), 786 (m), 736 (m), 700 (m), 684 (m), 601 (w) cm^{-1}. MS-EI: m/z = 633 [M$^+$ − 1].

(*Z*)-$Cp^*_2Ti(H)(N(SiHPh_2)(N{=}C(H)C_6H_4Me)$ ((*Z*)-20). To a solution of **8** (190 mg, 0.422 mmol) in C_6H_6 (15 mL) was added Ph_2SiH_2 (78 mg, 0.422 mmol). The solution was stirred for 17 days at room temperature, during which time the solution turned from green to yellow. The volatile materials were removed under vacuum, and the

yellow powder was dissolved in ether (1.0 mL) and cooled to −50 °C to yield (*Z*)-**20** as yellow crystals (139 mg, 52%). ^{1}H NMR (C_6D_6): δ 8.37 (s, 1 H), 8.10 (m, 4 H), 7.50 (d, J = 7.8, 2 H), 7.24 (m, 6 H), 7.03 (d, J = 7.8, 2 H), 6.21 (s, J_{HSi} = 201.0, 1 H), 3.89 (s, 1 H), 2.15 (s, 3 H), 1.82 (s, 30 H) ppm. ^{13}C{^{1}H} (C_6D_6): δ 136.9 (C), 136.5 (CH), 133.8 (CH), 132.7 (C), 129.8 (CH), 128.9 (CH), 128.0 (CH), 126.1 (CH), 114.6 (C), 20.4 (CH_3), 12.6 (CH_3) ppm. IR (C_6H_6): 2999 (m), 2976 (m), 2947 (m), 2902 (m), 2874 (m), 2857 (m), 2140 (m), 2094 (w), 1589 (w), 1532 (w), 1429 (m), 1376 (m), 1122 (m), 1108 (m), 971 (m), 937 (m), 843 (s), 811 (m), 787 (m), 736 (m), 699 (m), 591 (m) cm^{-1}. MS-EI: m/z = 633 [M$^+$ − 1]. Anal. Calcd for $C_{40}H_{50}N_2SiTi$: C, 75.68; H, 7.94; N, 4.41. Found: C, 75.36; H, 7.98; N, 4.18.

Cp*$_2$Ti(NCO)N=C(H)C$_6$H$_4$Me) (21). To a solution of **8** (371 mg, 0.824 mmol) in C_6H_6 (20 mL) in a 100 mL bomb was added an atmosphere of CO. The solution was stirred for 2 days at room temperature, during which time the solution turned from green to orange to yellow. The volatile materials were removed under vacuum, and the resulting yellow powder was washed with pentane (2 × 8 mL) and dissolved in ether (12 mL). The ether solution was cooled to −50 °C to yield **21** as yellow crystals (341 mg, 86.5%). ^{1}H NMR (C_6D_6): δ 8.64 (s, 1 H), 7.58 (d, J = 7.9, 2 H), 7.07 (d, J = 7.9, 2 H), 2.02 (s, 3 H), 1.69 (s, 15 H) ppm. ^{13}C{^{1}H} NMR (C_6D_6): δ 155.2 (CH), 140.3 (C), 135.3 (C), 130.1 (CH), 127.5 (CH), 120.6 (C), 119.2 (C), 21.3 (CH_3), 11.8 (CH_3) ppm. IR (Nujol): 2215 (s), 1646 (m), 1611 (w), 1574 (w), 1529 (w), 1511 (w), 1497 (w), 1457 (m), 1438 (w), 1376 (w), 1307 (w), 1289 (w), 1173 (w), 1123 (w), 1110 (w), 1043 (w), 1021 (w), 811 (m), 791 (w) cm^{-1}. MS-EI: m/z = 478 [M$^+$]. Anal. Calcd for $C_{29}H_{38}N_2OTi$: C, 72.79; H, 8.00; N, 5.85. Found: C, 72.73; H, 7.76; N, 5.81.

X-ray Structure Determinations. X-ray diffraction measurements were made on a Siemens SMART (Siemens Industrial Automation, Inc.) diffractometer with a CCD area detector using graphite monochromated Mo Kα radiation. The crystal was mounted on a glass fiber using Paratone N hydrocarbon oil. A hemisphere of data was collected using ω scans of 0.3°. Cell constants and an orientation matrix for data collection were obtained from a least squares refinement using the measured positions of reflections in the range $3.00 < 2\theta < 45.00°$. Frame data were integrated using the program SAINT (SAX Area-Detector Integration Program; V4.024; Siemens Industrial Automation, Inc.: Madison, WI, 1995). Empirical absorption corrections, when needed, were based on measurements of multiply redundant data and were performed using the programs XPREP (part of the SHELXTL Crystal Structure Determination Package; Siemens Industrial Automation, Inc.: Madison, WI, 1995) or SADABS. Equivalent reflections were merged. The data were corrected for Lorentz and polarization effects. A secondary extinction correction was applied if appropriate. The structures were solved using the teXsan crystallographic software package of the Molecular Structure Corp., using direct methods[69,70] and expanded using Fourier techniques.[71] All non-hydrogen atoms were refined anisotropically, and hydrogen atoms were included in calculated positions but not refined unless otherwise noted. The function minimized in the full-matrix least squares refinement was $\Sigma w(|F_o| - |F_c|)^2$. The weighting scheme was based on counting statistics and included a factor to downweight the intense reflections. Crystallographic data are summarized in Tables 1 and 5. Positional and anisotropic thermal parameters, tables of bond lengths and angles, and complete crystal and data collection parameters are provided as Supporting Information.

(a) For 5. Crystals were grown by slow cooling of a toluene solution of **5** to −50 °C. The systematic absences of *h*0*l*, $h + l \neq 2n$, and 0*k*0, $k \neq 2n$, uniquely determined the space group to be $P2_1/n$ (No. 14). No decay correction or absorption correction was applied. All non-hydrogen atoms except the minor component of the disorder of the ligand were refined anisotropically; those two atomic positions were refined isotropically.

(b) For 9. Crystals were grown by slow cooling of a toluene solution of **9** to −50 °C. Based on the systematic absences of *hkl*, $h + k \neq 2n$, and *h*0*l*, $l \neq 2n$, packing considerations, a statistical analysis of intensity distribution, and the successful solution and refinement of this structure determined the space group was determined to be $Cmc2_1$ (No. 36). No decay or absorption correction was applied. Some non-hydrogen atoms were refined anisotropically, while the rest were refined isotropically.

(c) For 17. Crystals were grown by slow cooling of a toluene solution of **17** to −50 °C. On the basis of a statistical analysis of intensity distribution, and the successful solution and refinement of the structure, the space group was determined to be $P\bar{1}$ (No. 2). An empirical absorption correction (T_{max} = 0.90, T_{min} = 0.73) was applied.

(d) For (*Z*)-19. Crystals were grown by slow cooling of a ether solution of (*Z*)-**19** to −50 °C. The systematic absences of *h*0*l*, $h + l \neq 2n$, and 0*k*0, $k \neq 2n$, uniquely determined the space group to be $P2_1/n$ (No. 14). No decay correction was applied. An empirical absorption correction (T_{max} = 0.93, T_{min} = 0.80) was applied. Some hydrogen atoms were refined isotropically; the rest were included in fixed positions.

(e) For 21. Crystals were grown by slow cooling of an ether solution of **21** to −50 °C. The systematic absences of *h*0*l*, $h + l \neq 2n$, and 0*k*0, $k \neq 2n$, uniquely determined the space group to be $P2_1/n$ (No. 14). No decay or absorption correction was applied.

Acknowledgment. We thank the National Institutes of Health (Grant No. GM-25459) for generous financial support of this work and Mr. Jeffrey Golden for a sample of Np_3Al. We are grateful to Dr. F. J. Hollander, director of the University of California Berkeley College of Chemistry X-ray diffraction facility (CHEXRAY), and Dr. Ryan Powers for solving the crystal structures of **5**, **9**, **17**, (*Z*)-**19**, and **21**.

Supporting Information Available: Tables of positional and thermal parameters, intramolecular bond lengths and angles for the structures of **5**, **9**, **17**, (*Z*)-**19**, and **21**, and measured and calculated (E/C Method) rate constants for the reaction of **5**−**9** with styrene and figures of HMQC spectrum for **9** and NOESY and HMQC spectra for **14** (44 pages, print/PDF). See any current masthead page for ordering information and Web access instructions.

JA981340B

(69) Hai-Fu, F. *SAP191, Structure Analysis Programs with Intelligent Control*; Rigaku Corp.: Tokyo, Japan, 1991.

(70) Altomare, A.; Cascarano, G.; Giacovazzo, C.; Guagliardi, A. *J. Appl. Crystallogr.* **1993**, *26*, 343.

(71) Beurskens, P. T.; Admiraal, G.; Beurskens, G.; Bosman, W. P.; Garcia-Granda, S.; Gould, R. O.; Smits, J. M. M.; Smykalla, C. *DIRDIF92, The DIRDIF program system;* Technical Report of the Crystallographic Laboratory, University of Nijmegen: Nijmegen, The Netherlands, 1992.